

PRACTICAL APPLICATIONS OF ROTORDYNAMICS, BEARING DESIGN, MECHANICAL ANALYSIS, AND VIBRATION DIAGNOSTICS TO DESIGN PROBLEMS OF ROTATING MACHINERY IN OPERATION

by

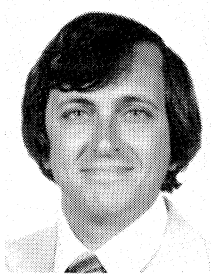
John Mirro

Vice President

Machinery Vibration Specialist

Connec, Incorporated

Allentown, Pennsylvania



John Mirro is Vice President and Machinery Vibration Specialist for Connec, Incorporated, in Allentown, Pennsylvania, and is responsible for the analysis, design, and troubleshooting of new, existing, and rerated high performance rotating machinery. He has over 20 years experience in rotorbearing system design.

Prior to his cofounding Connec, Mr. Mirro was Supervisor of the Rotordynamics Analysis Group for the Turbomachinery Division, Ingersoll-Rand Company. In this capacity, he was responsible for the design of rotating system components for pumps, compressors, turbines, expanders, gears, and motors.

Previous to his joining Ingersoll-Rand Company, Mr. Mirro was Design Engineer for Sikorsky Aircraft, United Technologies Group. He also worked for NASA at the Charles Stark Draper Laboratories on the rotor controls for the space shuttle RMS system under the auspices of NSF and AEC.

Mr. Mirro graduated Summa Cum Laude from Lehigh University with a B. S. degree in Engineering Mechanics in 1971. He is also a 1972 graduate of the Massachusetts Institute of Technology with an M. S. degree in Mechanical Engineering. He is a member of ASME, the Vibration Institute, ROMAC, and contributes to API. Several honorary societies have elected him to membership including Phi Beta Kappa, Pi Tau Sigma, Tau Beta Pi, and Sigma XI.

ABSTRACT

A large majority of today's existing high performance rotating machinery in operation was manufactured and installed long before the advent of powerful design tools in the complex areas of rotor system dynamics and stability as well as the exacting science of hydrodynamic bearing design. Not having had the advantage of modern automated analysis techniques and their associated technologies, many of today's critical pieces of turbomachinery are experiencing operational difficulties which are symptomatic, not of maintenance related problems, but of basic inadequacy of design. Furthermore, some marginal machines operate satisfactorily until they are rerated, but then require mechanical upgrade. Other problems result from the use of poorly designed aftermarket or OEM parts. Some units can be optimized for future operational reliability while others can be analyzed for rapid solution of potential future problems.

Various case histories relevant to design deficiencies of rotating machinery in operation are documented.

INTRODUCTION

A vast majority of today's high performance rotating machinery population, that great body of engineered equipment upon which industry depends to maintain current production levels or to meet greater demands by enhancing performance via machinery upgrades, was manufactured and installed long before the advent of powerful design tools in the complex areas of rotor system dynamics and stability along with the exacting science of hydrodynamic bearing design. The emerging technologies of the mid-1970s to the present have offered rotating machinery engineers of the last decade a far better understanding of the essentials of successful machinery design for acceptable machine dynamics and vibration control along with optimum turbo rotor mechanical performance.

Not having had the advantage of modern automated analysis techniques and their associated technologies, many of today's critical pieces of turbomachinery are experiencing operational difficulties which are symptomatic not of the maintenance problems which they are being treated as, but are symptomatic of a more fundamental shortcoming *inadequacy of the design*. Furthermore, some critical machines operate satisfactorily with a marginal design (relative to the rotor system) until they are rerated to yield greater performance—power, speed, efficiency, energy density, etc. The rerated or upgraded units are capable of improved performance characteristics but are no longer capable of acceptable and reliable mechanical operation. Redesign of the mechanical package (rotor, bearings, seals, couplings, supports, etc.) may be required in order to produce an acceptable design relative to meeting industry-wide design standards and acceptance criteria, and at the same time minimizing unit downtime and high maintenance costs.

Other areas of machinery operational problems include those instances where aftermarket replacement parts or redesigned retrofit parts, or OEM parts have been provided which are substandard in design or improperly designed. Furthermore, the importance of manufacturing tolerances and quality control for rotor system replacement parts (such as bearings, seals, rotating assembly parts, etc.) and their impact on machine vibration levels and overall unit mechanical integrity is not always appreciated. Some pieces of critical turbomachinery may have experienced none of the aforementioned difficulties. Yet, if subjected to a detailed design audit and comprehensive engineering review, the machinery can be brought up to modern day standards of mechanical design, sometimes at very little expense and with minor modification, and yielding great returns in future operational reliability for the existing or rerated unit. Additionally, some machines may require no retrofit or rework at all. Simply knowing the predicted dynamic behavior of a rotating machine can provide an invaluable knowledge base for future operating experiences with the unit, in terms of understanding and expedient resolution of operating problems, once

again minimizing costly downtime and unnecessary maintenance expense.

Eight significant case histories of importance to the discussion of machinery design deficiencies are documented. These examples of turbomachinery analysis and design problems were among many encountered recently. They represent a cross section of the variety and subtlety of design problems encountered in existing rotating machinery and the engineering resolutions, including upgrade and redesign.

CASE STUDY 1

Gas Plant Forced Downtime Due to Gearbox High Vibration Shutdown of Multiple Geared Power Turbine/Compressor Sets

Problem Definition

The high vibration excursions of the low speed and high speed gearshafts occurred at the time of the gas plant (Figure 1) turnaround which included replacement of the existing gearbox internals - gears and bearings - as part of an overall performance rerate as well as mechanical upgrade. The scope of the project required a complete engineering study including a rotor-dynamics analysis, and in conjunction with unit vibration monitoring and analysis as well as experience in diagnosing gearbox high vibration problems, a successful resolution of the gear vibration problem was achieved. Elements of the problem and its solution included:

- removal of excessive gear transmission error due to very poor tooth finish.
- removal of excessive gear pitchline eccentricity and resultant runout.
- consideration of unbalance and misalignment.
- modification of radial bearing inserts to proper running clearances and a stabilized multipocket bore design in order to reduce 1X vibration levels and stabilize possible fractional frequency components, respectively.
- low level excitation of the fundamental torsional critical speed of the train.

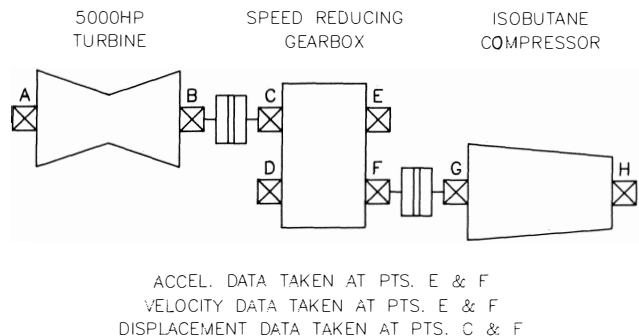


Figure 1. Machinery General Arrangement and Instrumentation.

This complex and multifaceted machinery problem was resolved in a very expedient manner, due to a proper blend of rotor-dynamics analysis, machinery vibration monitoring and signature analysis, and practical experience with gear vibration diagnostics.

History of Events

Vibration Data Acquisition

Upon attempting to restart the isobutane units, high level vibration was experienced on all units and continuous operation

was not possible. All gears were fully instrumented in order to collect transient startup vibration data in the form of:

- shaft displacement data (Figure 2).
- bearing cap velocity data (Figure 3).
- bearing cap acceleration data (Figure 4).

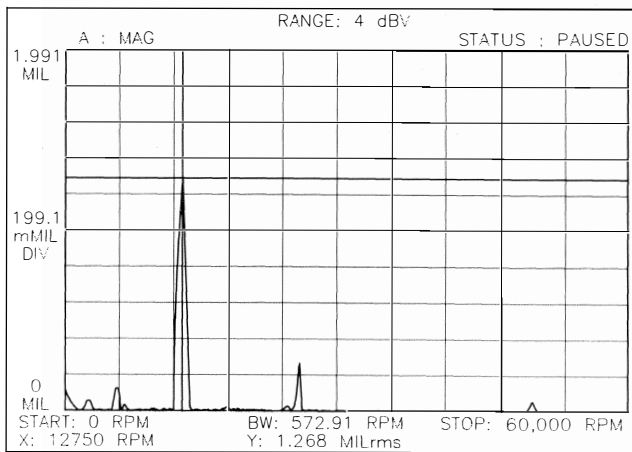


Figure 2. High Speed Pinion Shaft Displacement Spectrum.

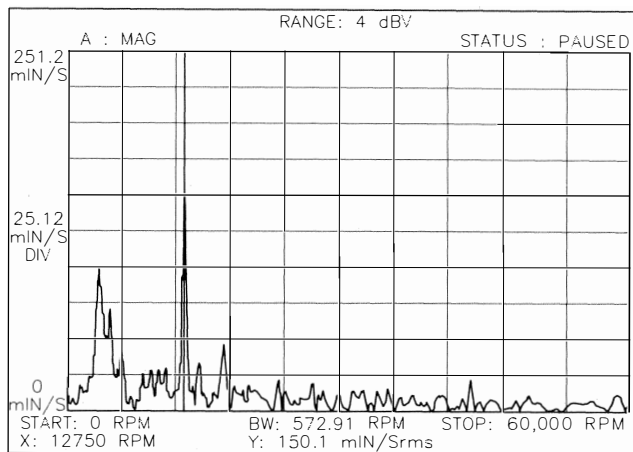


Figure 3. High Speed Pinion Bearing Cap Velocity Spectrum.

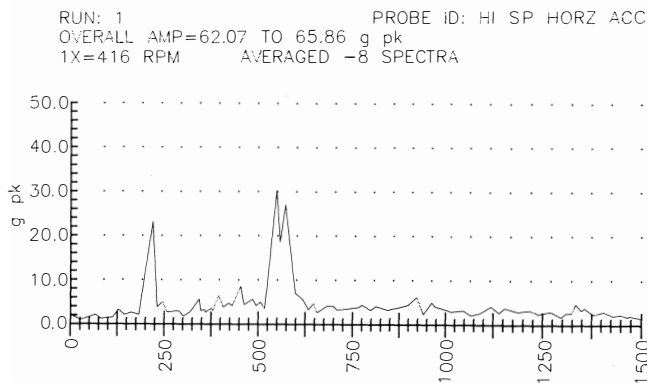


Figure 4. High Speed Pinion Bearing Cap Acceleration Spectrum.

Collection of vibration data was carried out for all gearboxes during short duration runs at steady state conditions and normal

running speed, 15,000 rpm high speed shaft and 6,000 rpm low speed shaft. Analysis of this data indicated all units exhibited vibration components at the following various frequencies (Figures 2, 3, 4).

- Subsynchronous, 40 to 50 percent components, low level vibration
- Synchronous, high vibration, 1.5 to 2.0 mils
- Supersynchronous harmonics, very low level vibration
- Gear meshing frequency, very high acceleration components, 30 to 60 Gs at approximately 600,000 cpm
- Subharmonics and superharmonics of meshing frequency, very high level, e. g., 30 Gs at 180,000 cpm
- Gear sideband frequencies, high level synchronous speed sidebands of the subharmonics and superharmonics of gear meshing frequency

The gearboxes, thus, were found incapable of continuous operation due to high level synchronous vibration and frequency acceleration components related to gear meshing frequencies, and associated high noise levels.

Vibration Analysis

The vibration response of the gearboxes was very complex and a rapid solution to the problem was required. The frequency content of the displacement, velocity, and acceleration spectrums obtained for both low and high speed gear shafts on all units is summarized in Table 1. Also summarized in Table 1 are the probable root causes of the respective vibration components based on:

- Gearshaft critical speed analysis.
- Residual unbalance response analysis.
- Rotor-bearing system stability analysis.
- Train torsional critical speed analysis.
- Bearing design analysis.
- High speed gear diagnostics.

Table 1. Gearbox Vibration Component Frequencies and Probable Causes.

$\frac{N}{2}$ -Approx. Half Speed	N (LS+HS) Synchronous Speed	2N,3N...nN Harmonics	$\frac{F}{n}$ Gear Meshing Frequency	$\frac{F}{n} \dots nF$ Harmonics	$\frac{F}{n} \pm N \dots nF \pm N$ Sidebands
<i>Probable Cause:</i>	<i>Probable Cause:</i>	<i>Probable Cause:</i>	<i>Probable Cause:</i>	<i>Probable Cause:</i>	<i>Probable Cause:</i>
Fundamental torsional critical speed of the train	Unbalance Reduction in critical speed of high speed shaft due to soft support	2N-Misalignment 3N...nN (N<10) Non-rotating looseness	Transmission error (poor tooth finish) Pitch line runout	Transmission error Pitch line runout	Pitch line runout
Low Sommerfeld gearshaft instability	Pitch line runout Faulty tooth		Misalignment		

The system analysis indicates that possible reasons for the high vibration include:

- gear transmission error due to unacceptable gear tooth surface finish and/or unacceptably high pitch line runout resulting in high level high frequency components as manifested by bearing cap G-levels.
- misalignment, unbalance, or faulty tooth, giving rise to high running speed and harmonic components.
- reduction in the rotor critical speed of the high speed pinion, which was located at 115 percent of operating speed for maximum continuous operating speed (MCOs), due possibly to a "soft support" reduction in frequency, and resulting in high synchronous vibration.

- low Sommerfeld gearshaft bearing instability, which was predicted by the bearing design analysis to yield possible subsynchronous vibration.
- reexcitation of the fundamental torsional critical speed of the train, which occurred subsynchronously and at approximately N/2 for the low speed unit.

Corrective Actions Taken

• Cold and hot checks indicated misalignment was not a problem. Certified balance records gave a good confidence level that the rotors were balanced to specification. In addition, the synchronous vibration bodé plots showed no indication of a speed squared effect which would show the presence of a high residual unbalance. Unbalance or misalignment problems were thus dismissed.

• The single helical gears were removed from Unit 3 and sent back to the manufacturer to be checked for mechanical integrity and manufacturing accuracy. It was determined upon inspection that total indicated pitchline runout was in the range of 0.003 to 0.004 in, indicating very high gear profile accumulated manufacturing error for the hobbled and shaved gears. An attempt at rework was unsuccessful, so the gears were sent to another shop to be improved via grinding. This operation was successful.

• It was also noticed upon initial inspection that the gear tooth surface finish was, mysteriously, far worse than the expected norm for gears that have not been ground. This condition was improved during rework on the grinding machine. Although gear mesh remachining resulted in greater operating gear backlash, the final backlash was well within the manufacturer's normal design standards for acceptance, in the range of 0.012 to 0.014 in total.

• Reassembly of the unit and subsequent restart resulted in the following unit vibration:

- greatly reduced mesh frequency components, 5.0 to 10 Gs
- greatly reduced mesh frequency harmonics, 1.0 to 5.0 Gs
- greatly reduced mesh frequency sidebands, low level

The gears also ran quietly. However, the synchronous speed vibration levels were only slightly reduced from their original high levels of almost 2 mils. Also, low level components at subsynchronous vibration still persisted.

• The possibility of running in resonance due to a soft support was addressed since rotor balance was perceived to be good. The new gearbox bearings were removed, inspected, and found to have excessive clearance. The high speed shaft journal diameters are D = 3.250 in while clearances were measured at 0.011 to 0.012 in (diametral). The low speed shaft journal diameters are D = 3.500 in, while clearances were measured at 0.007 to 0.008 in (diametral). These bearings were a plain cylindrical insert design with two axial oil feed grooves located on the horizontal parting line. It was decided to modify the design to:

- proper (tighter) design clearances to resolve the high synchronous vibration problem. Analysis indicated optimum clearance at 0.005 to 0.006 in (diametral) for both high and low speed journal bearings.
- double pressure-pocket design (Figure 5) to replace the plain bushing design in order to reduce or eliminate the possible instability response at subsynchronous frequency (approximately 45 percent) as predicted and measured.
- Reassembly of the unit (with now reworked gears and journal bearings) and subsequent restart resulted in the following unit vibration:
 - greatly reduced synchronous speed vibration, 0.5 mil
 - slightly reduced subsynchronous vibration, low level

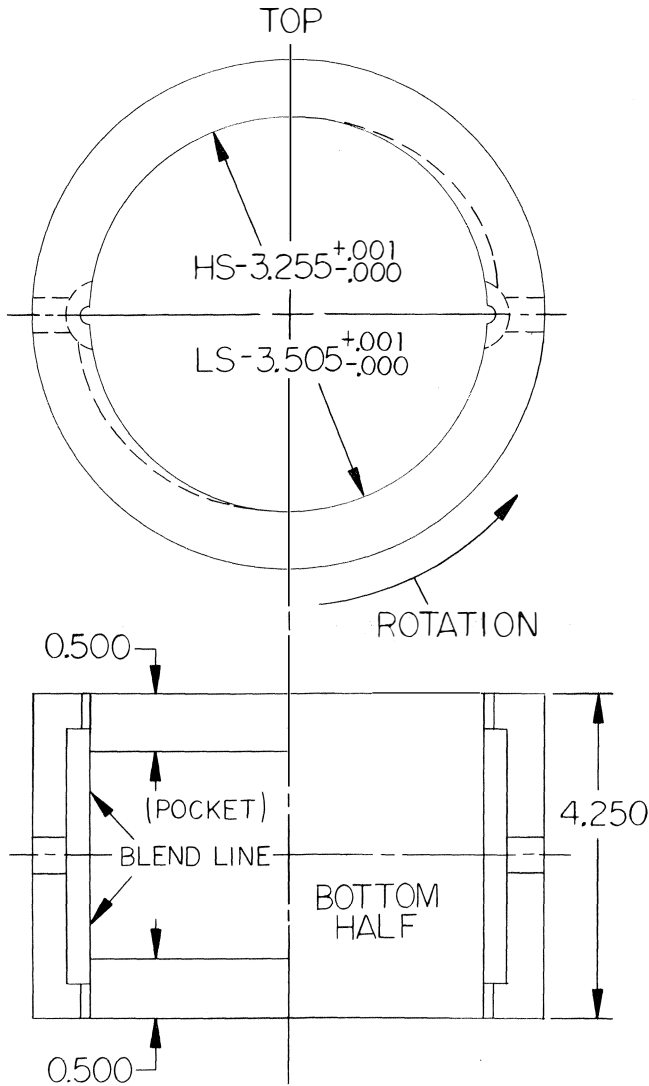


Figure 5. Redesign Double-Pocket Gearbox Bearings.

- further reduced mesh frequency components, three to eight Gs
- further reduced mesh frequency harmonics, one to three Gs

All vibration frequency components were now reduced to normal and acceptable amplitude levels. The remaining low level subsynchronous vibrations were verified through further testing to indeed be a reexcitation of the fundamental train torsional critical speed, which yielded acceptable low level shaft stresses and was not of concern.

The end result was an operationally excellent gearbox. All units were reworked in the same manner. During this process it was required to utilize some established guidelines for acceptable bearing housing vibration, particularly with respect to the high frequency gearmesh components being measured with case mounted accelerometers. Lifson, Simmons, and Smalley [1] suggest vibration limits for rotating machinery based on a comprehensive evaluation of statistical or empirical data from a wide variety of operating units. To each class of machine certain correction factors are then applied to overall vibration levels to arrive at an acceptance criterion as reproduced in Figure 6.

When the final bearing housing G-levels for the present gearboxes are corrected for:

- stiff shaft behavior, $K_1 = 0.7$
- high-frequency gear vibration, $K_2 = 0.35$

The end result is operation in the acceptable (B) to as-new (A) regions of Figure 6.

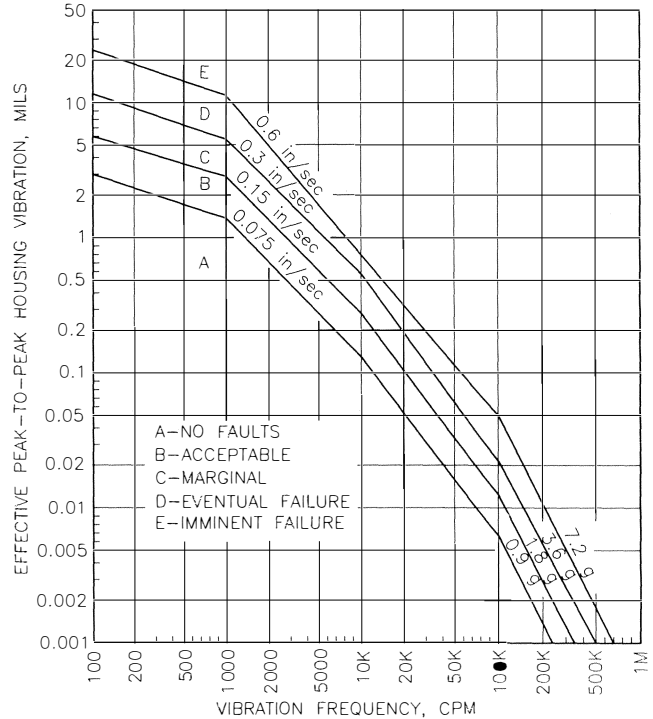


Figure 6. Effective Vibration Limits for Housings [1].

Conclusions

- The subject gears exhibited a complex frequency spectrum of high vibration components and required a blend of:
 - rotordynamics analysis.
 - machinery vibration monitoring and signature analysis.
 - practical experience with gear vibration diagnostics to arrive at an expedient solution of the problem to minimize downtime and lost production.

High frequency gearmesh diagnostics must be done with transducers that are capable of high frequency response such as case mounted accelerometers, and as such can serve an important role in confirming the integrity of meshing gears relative to such specifics as:

- pitchline runout or nonconcentricity with the shaft journals.
- gear transmission error due to poor tooth surface finish.
- other tooth fault or gearing errors.

In this case, very high pitch line runout, 0.003 to 0.004 in, showed no indications on the shaft vibration probes, but case acceleration levels were as high as 60 Gs.

This is one of many examples of high synchronous vibration caused by an inadequate component design rather than the more customary reasons of unbalance, misalignment, looseness, or wear, i. e., maintenance related problems. In this case, a new hydrodynamic bearing was originally supplied with design clearances which exceeded twice the normally accepted running clearances for similar applications. Additionally, subsequent

analysis clearly demonstrated the advantages of designing with a stabilized bearing insert (Figure 5).

CASE STUDY 2

Performance Rerate and Mechanical Design Optimization of the Gas Compressor of Case Study 1

Problem Definition

This isobutane compressor not only had a history of downtime due to mechanical failure (thrust bearings, radial bearings, couplings, gears) but was also in the process of being rerated to conditions of higher efficiency and flow, requiring somewhat higher speed and power consumption. These requirements resulted in the need for a complete redesign of the unit's journal bearings for successful and reliable operation. Elements of the problem and its solution included:

- replacement of the existing axially-tapered plain insert bearings with an optimized single pressure-dam insert bearing design with no axial taper.
- shifting the rotor critical from 4000 rpm to 8000 rpm through improved stiffness and damping from the lightly loaded journal bearings.
- enhancement of overall rotor-bearing system stability by raising the onset of instability from 6,000 rpm to 14,000 rpm, which was critical to the success of the compressor rerate. This instability phenomenon, it was later determined, plagued the OEM, who offered a three-taper land stabilized bearing insert as a retrofit to similar existing units.
- demonstration that the new optimized pressure dam bearing design, lacking the axial taper, offered greater reliability and wear characteristics in terms of improved minimum oil film thickness, reduced operating temperature, ability to meter flow and thus maintain lube system pressure, and improved lube oil flow and distribution.

Results of the Rotor Bearing System Dynamics Analysis

Isobutane Compressor with Existing Axial Taper Bore Bearing Design (Figure 7)

Isobutane Compressor with Optimized Pressure Dam Bearing Design (Figure 8)

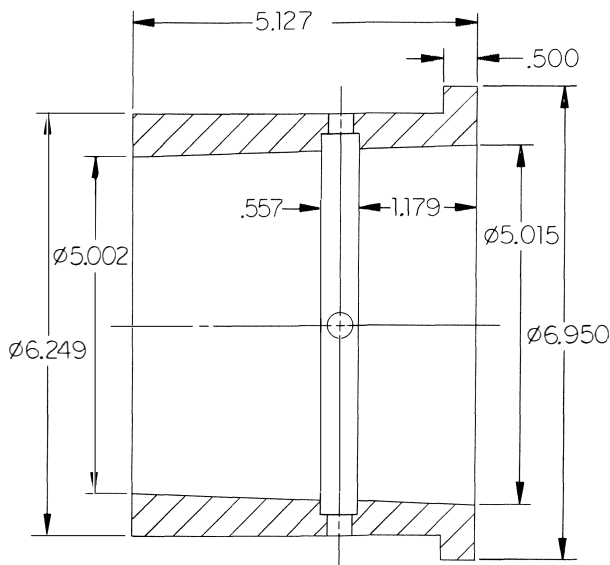


Figure 7. Existing Axial Taper Bore Bearing Design.

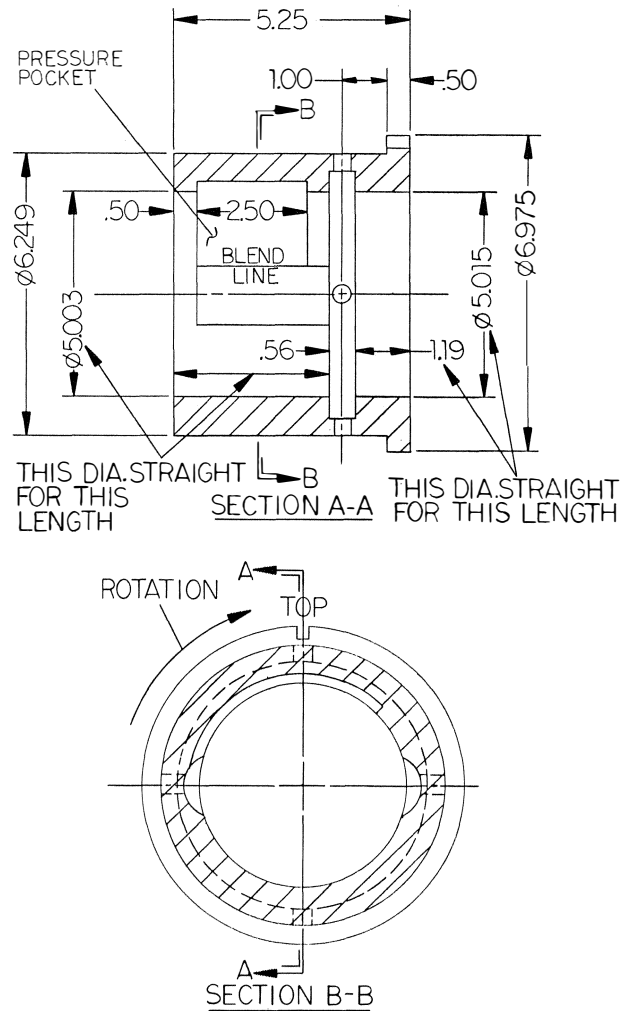


Figure 8. Redesigned Straight Bore Pressure-Dam Bearing.

Undamped Critical Speed Analysis

As shown in the rotor undamped critical speed map (Figure 9), the first rigid bearing critical of the compressor is located above the operating range at $N_{cr} \sim 10,000$ cpm.

The second bearing critical (conical mode shape, stiff rotor) is critically damped and, therefore, is not a factor in the resonant vibration of this machine for either the old axial taper bore bearings or the new pressure dam bearings.

The second actual critical for the machine is its first free-free mode (third critical) located in frequency at $N_{FF} \sim 23,000$ cpm for both old and new bearing designs.

As can be seen in Figure 9 from the intersection of the first critical (cylindrical mode shape) with the horizontal and vertical bearing stiffness loci for both old and new bearing designs, the compressor traverses the first critical below normal running speed with the old bearing design. Dynamic response analysis will confirm this fact with the damped first critical predicted to amplify between $N_{c1} = 4,000$ rpm to 5,000 rpm.

The critical speed map for the new optimized pressure-dam bearing design indicates the rotor's first critical to lie above the running speed range. Dynamic response analysis will confirm that with the much improved stiffness characteristic of the new bearing design, coupled with dynamic stiffening due to much improved damping (Table 2), the first critical will amplify be-

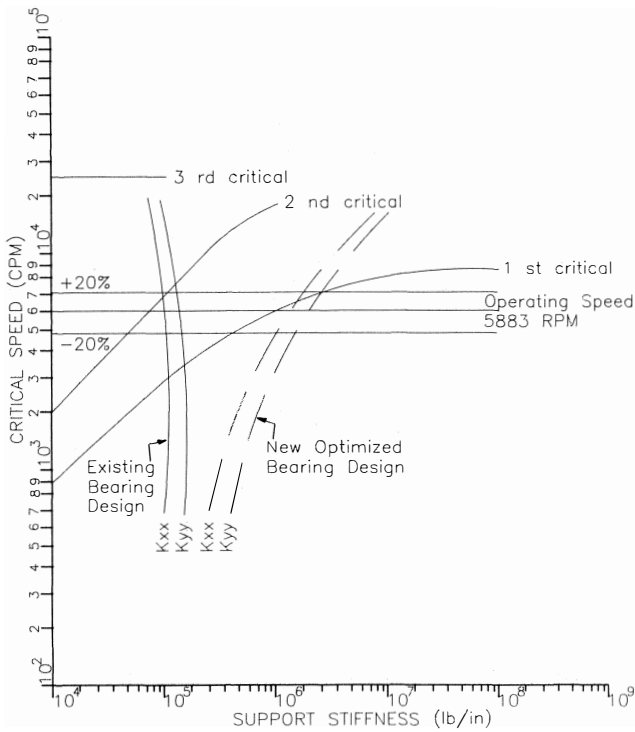


Figure 9. Undamped Critical Speed Map of the Isobutane Compressor.

tween $Nc1 = 8,000$ rpm to $9,000$ rpm. This provides an average separation margin of 30 percent above the operating range, with the vibration response showing well-damped behavior.

Especially significant is the fact that the new bearing design results in the compressor becoming a true stiff shaft design, i. e., one that operates below its first critical speed, a very desirable

Table 2. Summary of the Rotor Bearing System Design Optimization for an Isobutane Compressor.

Design Parameter	Compressor With Existing Taper Bore Bearing	Compressor With Optimized Pressure Dam Bearings
K_{xx} (@ 5883 rpm)	144,000 lb/in	1,000,000 lb/in
K_{yy} (@ 5883 rpm)	121,000 lb/in	1,190,000 lb/in
C_{xx} (@ 5883 rpm)	678 lb-sec/in	2,800 lb-sec/in
C_{yy} (@ 5883 rpm)	916 lb-sec/in	6,572 lb-sec/in
First Critical, $Nc1$	4,000-5,000 cpm	8,000-9,000 cpm
Second Critical, $Nc2$	23,000 cpm	23,000 cpm
Vibration (@ 5883 rpm) (Coupling End Bearing)	0.16 mils/oz-in	0.08 mils/oz-in
Vibration (@ 5883 rpm) (Thrust End Bearing)	0.11 mils/oz-in	0.09 mils/oz-in
% Vibration (@ 5883 rpm) (Coupling End Bearing)	100%	50%
% Vibration (@ 5883 rpm) (Thrust End Bearing)	100%	82%
δ_{n1} , Base Log Dec	+0.161	+2.670
Threshold of Instability (Unstable Speed)	6150 rpm	14,000 rpm
Non-Synchronous A.F.	19.5	1.39
Instability Frequency	3070 cpm	4010 cpm

*A.F. = Amplification Factor

ble situation relative to machinery vibration. It is this stiff shaft characteristic that results in the hydrodynamic bearing design being dominant in the overall machine dynamics.

It is significant to note that the bearing stiffness characteristic shown in Figure 9 for the old bearing design indicates unacceptably low bearing stiffness relative to good machine dynamics. This is particularly important relative to the extremely lightly loaded coupling side journal, unit load = 15 to 20 psi, which results in undesirable:

- dynamic response to unbalance—low restraint force
- rotor bearing stability—light load instability

Considerations of light load dynamic response and light load instability become increasingly significant as a unit is uprated in speed and/or power. The following dynamics and stability analysis will detail the great improvement in mechanical integrity of the gas compressor with the new optimized bearing design.

Rotordynamic Response to Residual Unbalance

The rotor-bearing system design summary (Table 2) tabulates a comparison of the fluid-film hydrodynamic stiffness and damping properties of the old and new radial bearing designs. The new bearing design offers an order of magnitude improvement in oil film stiffness and a four to seven factor of improvement in oil film damping. These impressive improvements in the operating characteristics of the compressor bearings are of great benefit to the rotordynamics, as shown in the following dynamics and stability analysis, due to the stiffness of the rotor.

The results are given in Figure 10 of the rotor unbalance response analysis for both the existing axial taper bore bearing design, along with the new pressure dam bearing design for $U = 4W/N$ oz-in unbalance.

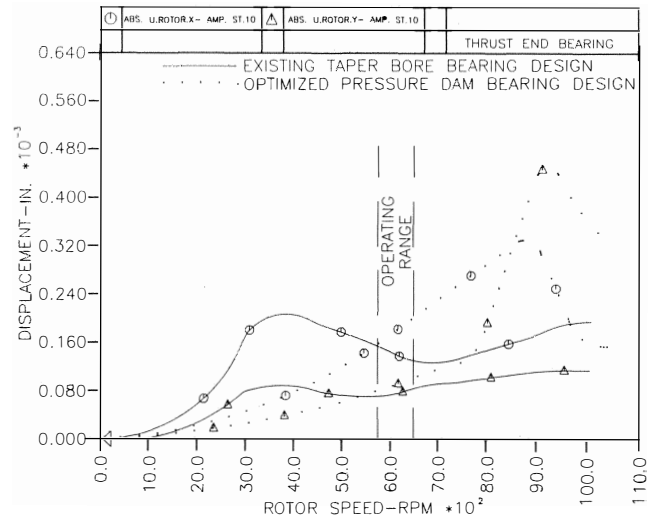


Figure 10. Rotor Unbalance Response for Existing and Redesigned Bearings.

For the old bearing design, the first critical is predicted to amplify between $4,000$ rpm to $5,000$ rpm, and it shows its most pronounced peak at the thrust end of the machine. Although the analysis predicts good damping, past operation near this critical has resulted in high vibration problems.

Vibration levels at the coupling end of the machine are not well-behaved, following a linear ramp-up with speed. This characteristic is indicative of the light load problem at the suction side bearing, in which sufficient stiffness and damping are not generated by the existing taper bore bearing inserts,

thereby allowing high level vibration excursions and rotor instability to occur.

For the new bearing design, the first critical is predicted to amplify between 8,000 rpm to 9,000 rpm, allowing the compressor to operate without passing through a rotor critical.

The greater hydrodynamic stiffness and damping generated by the new bearing design results in greatly reduced vibration levels experienced at the suction side of the machine. A comparison of calculated vibration levels and percent improvements are given in Table 2, where it is shown that, as compared with original vibration amplitudes, the new bearings result in:

- 50 percent improvement in vibration—suction side.
- 20 percent improvement in vibration—discharge side.

Rotor vibration response analysis thus shows a dramatic improvement with the new bearing design in terms of:

- critical speed frequency placement.
- operating range vibration levels.

Many years of operating experience with pressure-dam design bearings have proven their superiority for this class of stiff shaft rotor.

During the course of this analysis, it was demonstrated that the pressure dam bearings designed for this application are superior to an existing three-lobe standard replacement bearing design, which exists on the market as a retrofit to the existing axial taper bore bearing design. This especially applies to rotor-bearing system instability.

Rotor Bearing System Stability

The results of the compressor rotor bearing system stability analysis are given in Figure 11 for both old and new bearing designs.

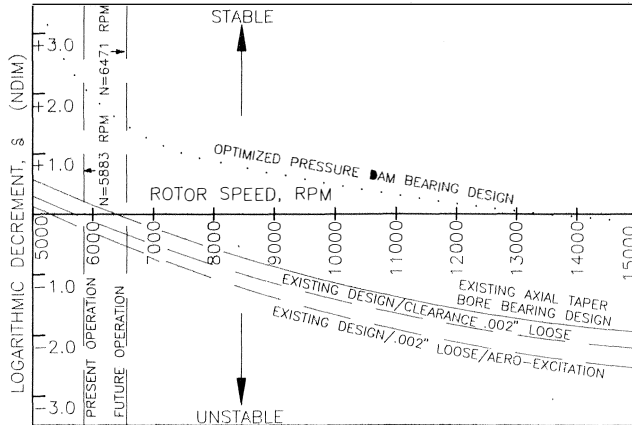


Figure 11. Rotor bearing System Stability for Existing and Redesigned Bearings.

The most significant aspect of the rotor vibration characteristic is its proximity to the threshold of instability with the old bearing design. As discussed above, this is due to extremely light journal loads, especially at the suction side bearing, in conjunction with undesirable journal bearing design characteristics.

Rotor-bearing stability analysis indicates a base log dec, $\delta_0 = + 0.161$ ($N = 5883$ rpm, no aeroexcitation) for the old bearing design.

A finite stability threshold exists for the old bearing design at about 6150 rpm, i. e., that speed at which the rotor could become unstable and experience unacceptably high levels of non-synchronous vibration, leading to potentially damaging vibration levels.

This instability speed could be further degraded (i. e., occur lower in speed) with the effects of (Figure 11):

- Aerodynamic Excitation, K_{xy} , on the rotor
- Manufacturing tolerances/errors on bearings
- Bearing clearance variations

The high mole weight gas makes aeroexcitation more likely to occur, i. e., a high energy density machine.

As this potential rotor instability exists for the present operating conditions, it was deemed advisable to retrofit the new optimized bearing inserts to existing machines as a product improvement. It would certainly also aid in reducing unbalance induced vibration, as well as eliminate the possibility of self-induced oil whirl in the bearings.

As the unit was uprated in speed and power, it became increasingly significant to utilize a stabilized bearing design with good dynamic characteristics. The new optimized pressure dam bearing design offers the much needed improvement.

Stability analysis indicates a base log dec, $\delta_0 = + 2.670$ ($N = 5883$ rpm, no aeroexcitation) for the new bearing design.

The stability threshold for the new bearing design exists at about 14,000 rpm, well removed from the operating speed range for the uprated rotor, and indicative of a highly stabilized bearing design with superior dynamic properties.

New Optimized Pressure Dam Bearing Design

This design (Figure 8) not only offers superior dynamic characteristics over the existing design, but offers equal or greater reliability and bearing life in terms of:

- wear.
- minimum oil film thickness exceeds 2.5 mils.
- reduced operating lube oil temperature.
- ability to maintain oil pressure in machine.
- proper oil flow rate throughput.
- ability to get oil to the bearing surfaces.

Conclusions

• The isobutane compressor with the existing taper bore bearing design has its first critical at:

$$Nc1 = 4,000 \text{ rpm} - 5,000 \text{ rpm}$$

The compressor with the new pressure dam bearing design has its first critical at:

$$Nc1 = 8,000 \text{ rpm} - 9,000 \text{ rpm}$$

• The shift in critical speed for the compressor is indicative of the much higher stiffness and damping generated by the new bearings thereby resolving the principal problem associated with the unit, i. e., that of lightly loaded journals.

• The new bearing design results in significantly reduced vibration levels due to rotor unbalance, where at running speed the following improvement is had:

- 50 percent improvement in vibration (suction side).
- 20 percent improvement in vibration (discharge side).

• The new bearing design results in great improvement in overall rotor-bearing system stability, where the improvement in raising the speed for the onset of instability is as follows:

- instability speed = 6,150 rpm (old bearing design)
- instability Speed = 14,000 rpm (new bearing design)

• The new bearing design offers greater reliability and wear characteristics in terms of improved minimum oil film thickness, reduced operating temperature, ability to maintain pressure, and improved lube oil flow and distribution.

• These improvements were critical to the successful performance rerate of the compressor, and the subsequent increase in power consumption and speed of the unit.

- Following the performance rerate and mechanical optimization of the bearing system, the unit was reinstalled, brought on-line, and subsequent operation showed high reliability to date with greatly reduced operating vibration levels and no indication of rotor instability.

CASE STUDY 3

Steam Turbine Rebuild and Redesign Study Uncovers the Cause of Past Frequent And Catastrophic Machine Failures

Problem Definition

The steam turbine (Figure 12) to be used as a driver for a high pressure barrel hydrogen recycle compressor application experienced in previous service frequent mechanical failures due to excessive machine vibration resulting in seriously damaged journal bearings, machine internals, and sometimes fire damage. This past history necessitated the requirement of a thorough engineering analysis prior to rebuild of the existing unit. Upon disassembly and inspection the existing journal bearing inserts, possibly not OEM parts, were found to be questionable relative to their general design and their ability to operate successfully in this (or any) machine. Elements of the problem and its solution included:

- replacement of the existing quasi-pressure-dam bearing inserts with an optimized 5-tilting shoe bearing design (Figure 13).
- demonstration that the existing bearing design violated numerous accepted standards of hydrodynamic bearing design of this type resulting in severe loss of load capacity.
- loss of hydrodynamic lubrication resulting in boundary lubrication at best and an unstable and unpredictable rotor.
- optimum dynamics and rotor stability with the redesigned journal bearings mandated for the turbine rebuild.

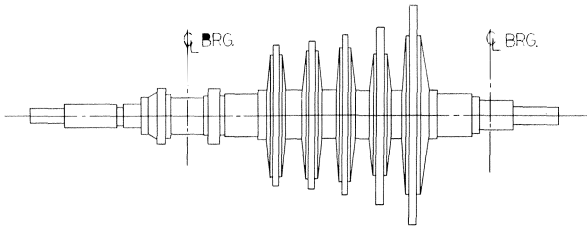


Figure 12. 4,000 HP Five-Stage Steam Turbine Rotor.

Design Critique of Existing Bearing Inserts

The existing highly modified pressure dam type bearing inserts (Figure 13) were not of a sound design for the following reasons:

The pressure step, although properly located at $Op = 135^\circ$ (from + X-axis), is heavily undercut to a depth of 0.045 to 0.050 in, which results in the inability of the dam to generate significant load, which is its principal purpose. A properly designed pressure-dam bearing would use an undercut depth of 3 to 6 times the bearing radial clearance, or 0.010 to 0.020 in, as shown in Figure 14, and as reported by Nicholas [2].

The pressure step is machined with a very short axial length, approximately 37 percent of the total bearing land length, and it is once again rendered ineffective. An optimum configuration would use $L = 65$ to 70 percent, as demonstrated by Nicholas [2].

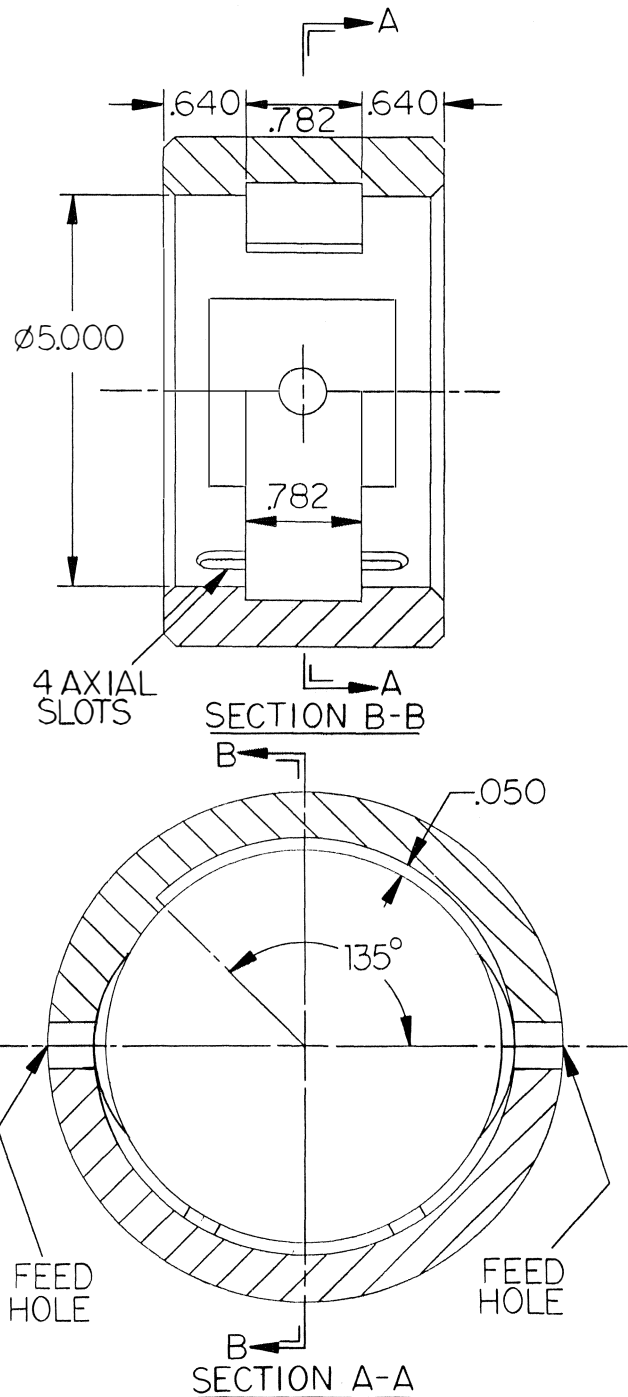


Figure 13. Existing Highly Modified Pressure-Dam Bearing.

The relief groove which runs along the full arc of the lower bearing half is very undesirable in that it separates the machine's actual bearing surfaces into two 5/8 inch wide strips, effectively running the machine on "knife-edges," resulting in an inadequate hydrodynamic film and the resultant loss of load capacity. (The purpose of a circumferentially grooved lower half bearing is typically to achieve higher unit journal load to enhance stability.)

Added to this are four milled axial slots in the lower bearing half which divide the two "knife-edges" into three segments each. This could possibly have been an attempt to get more oil

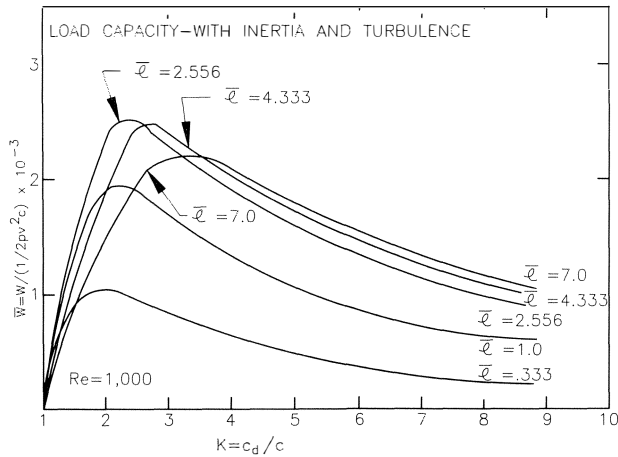


Figure 14. Stepped Slider Load Capacity [2].

to the bearing surfaces, but in reality serves to worsen an already inadequate design, relative to hydrodynamic load capability.

The existing bearing design violates numerous industry accepted standards of hydrodynamic bearing design of this type and the resulting lack of load capacity. The ability to sustain the rotor during normal operation on a hydrodynamic fluid film, avoiding bearing damage and allowing for smooth operation of the rotor, is expected and predicted by analysis (Figure 15).

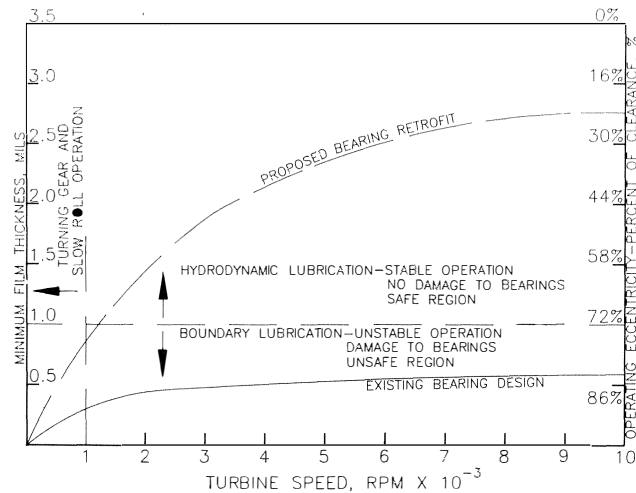


Figure 15. Minimum Oil Film Thickness of Existing and Retrofit Bearings.

The net result is the lack of hydrodynamic lubrication and the rotor operating with boundary lubrication at best. This leads to premature mechanical damage to bearing surfaces, excessive oil temperatures, high machine vibration, subsequent bearing failure, and possibly worse.

Results of the Rotor Bearing System Dynamics Analysis

Steam Turbine with Existing Pressure Dam Design

Steam Turbine with Optimized Five-Tilting Shoe Retrofit Bearing Design

Undamped Critical Speed Analysis. From the rotor undamped critical speed analysis, the first rigid bearing critical is located above the operating range at $N_{cr} = 11,500$ cpm.

The second bearing critical (conical mode shape, stiff rotor) is critically damped and therefore is not a factor in the resonant vibration of this machine for either the old pressure-dam bearings or the new five-tilting shoe bearings.

The steam turbine traverses the first critical below normal running speed with the existing bearings. Dynamic response analysis confirms this fact with the damped first critical predicted to occur between $N_{c1} = 3,000$ rpm to 4,000 rpm.

The obvious split between the horizontal and vertical bearing stiffness characteristics (Table 3) for the existing bearing design reflects the loss of load capacity (i. e., the ability to hold the rotor on a lubricant film without bearing damage) with the old design. For a lightly loaded journal such as this turbine, $W/LD = 40$ PSI, the bearing hydrodynamic characteristics should be symmetrical, as is evidenced by the X and Y characteristics of the new five-tilting pad bearings (Table 3).

Table 3. Hydrodynamic Bearing Coefficients—Steam Turbine Redesign.

Floating Ring Seal Characteristics @ No = 6000 rpm					
Startup Suction Pressure	Seal Eccentricity	Kxy (Lb/In)	Kyx (Lb/In)	Cxx (Lb-Sec) In	Cyy (Lb-Sec) In
Low (100 psig)	25%	-0-	-0-	-0-	-0-
Optimum (400 psig)	35%	123,000	-86,100	265	376
High (800 psig)	52%	319,000	-148,000	457	966

Relative to the immediately preceding discussion, dynamic response analysis confirms the loss of rotor damping and stability with the existing bearings, resulting in high amplification of the first critical. Alternately, dynamic response analysis also demonstrates the turbine with new tilt-pad bearings to be a true stiff shaft machine, with no amplification of machine criticals in the vicinity of the operating speed range, as the first and second criticals are critically damped.

It is significant to note that while the present analysis points out the tremendous improvement in mechanical integrity to be had with the proposed five-pad retrofit bearings, that improvement exceeds what can be shown here analytically. This is because the existing bearings have been conservatively analyzed without the short axial slots which were milled in the bottom half of the bearings. This unusual feature serves to further degrade the load capacity of these bearings—rendering the bearings incapable of supporting the rotor on a hydrodynamic film. The turbine probably operated on boundary lubrication at best in the past (Figure 15), thereby creating excessive bearing wear and damage, and in the event of major upset, would not have had the forgiveness of a rotor operating on a true hydrodynamic film. High lube oil temperatures and high machine vibration should be expected with the existing bearing design.

Especially significant is the fact that the new bearing design results in the steam turbine becoming a true stiff shaft design, i. e., one that operates below its first actual critical speed, a very desirable situation relative to machinery vibration and design.

Considerations of light load dynamic response and light load instability are documented in the following. The dynamics and stability analysis will detail the great improvement in mechanical integrity of the steam turbine with the new 5-shoe bearing design.

Rotordynamic Response to Residual Unbalance

The results of the rotor unbalance response analysis are given in Figure 16 for both the existing pressure-dam bearing design, and the new five-tilting shoe bearing design, for $U = 4W/N$ oz-in unbalance.

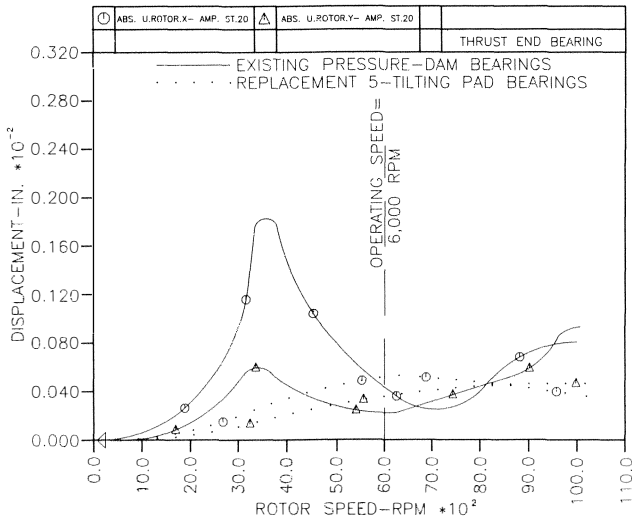


Figure 16. Rotor Unbalance Response for Existing and Replacement Bearings.

For the old bearing design, the first critical is predicted to amplify between 3,000 rpm to 4,000 rpm, and it shows its most pronounced peak at the thrust end of the machine.

Vibration levels at the coupling end of the machine are not well-behaved, following a linear ramp-up with speed. This characteristic is indicative of the combined light load/load capacity problem, in which sufficient stiffness and damping are not generated by the existing pressure-dam bearing inserts, thereby allowing high level vibration excursions and rotor instability to occur. This is worsened by the fact that actual behavior can be further degraded due to the lack of a hydrodynamic film.

For the new bearing design, the first mode is shown to be critically damped, allowing the turbine to operate without passing through a rotor critical.

As shown in Figure 16, the improved hydrodynamic stiffness and damping characteristics generated by the new bearing design result in a greatly improved vibration characteristic experienced by the machine.

Rotor Bearing System Stability

The results of the steam turbine rotor-bearing system stability analysis are given in Figure 17 for both old and new bearing designs.

It is significant to note the relative proximity to the threshold of instability with the old vs new bearing designs. As discussed previously, any turbine instability here is due to the light journal loads, in conjunction with undesirable journal bearing design characteristics, driven by any potential de-stabilizing forces.

Rotor/Bearing stability analysis indicates a base log dec, $\delta_o = + 0.420$ ($N = 6000$ rpm, no aeroexcitation) for the old bearing design. Stability analysis indicates a base log dec, $\delta_o = + 3.520$ ($N = 6000$ rpm, no aeroexcitation) for the new bearing design.

The stability threshold for the new bearing design is far superior to the existing bearing design and indicative of a highly stabilized bearing design with superior dynamic properties.

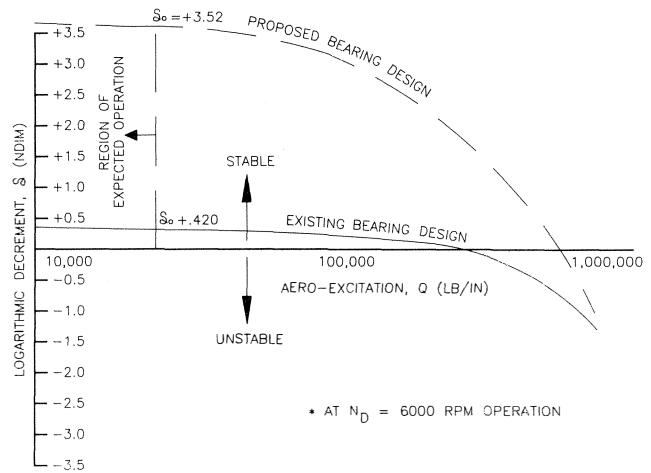


Figure 17. Steam Turbine Rotor Stability for Existing and Replacement Bearings.

Conclusions

- The five-tilting shoe replacement bearings for the steam turbine are demonstrated by this engineering study to be the superior choice for this application.

- The existing bearing design violates numerous accepted standards of hydrodynamic bearing design of this type resulting in a severe loss of load capacity. This prevents the bearings from sustaining hydrodynamic lubrication and results in the rotor operating with boundary lubrication at best.

- Actual operation with the existing bearing inserts is possibly worse than reported here since a lack of hydrodynamic lubrication results in an unstable and unpredictable rotor.

- The steam turbine with the existing pressure-dam bearing design has its highly amplified first critical at:

$$N_{c1} = 3,000 \text{ rpm to } 4,000 \text{ rpm}$$

The steam turbine with the new five-tilting shoe bearing design is shown to have a critically damped first mode, allowing the unit to operate without passing through a critical speed.

- The new bearing design results in great improvement in overall rotor-bearing system stability, where the improvement in rotor log dec is as follows:

- base log dec, $\delta_o = + 0.420$ (old bearing design)
- base log dec, $\delta_o = + 3.520$ (new bearing design)

CASE STUDY 4

Optimization of the Rotordynamics and Stability for The Compressor of Case Study 3 Through a “Modified Soft-Start”

Problem Definition

The eight-stage high pressure barrel hydrogen recycle compressor (Figure 18) whose driver is discussed in Case Study 3 operates on tilting-pad journal bearings and utilizes unequal pressure floating ring-type oil seals (Figure 19). This compressor was not a problematic machine in its past service, but it was desirable upon rebuild and unit packaging with the steam turbine discussed above to optimize its performance relative to predicted rotor unbalance response as well as rotor-system stability level. In service pressure levels experienced by the unit are in the neighborhood of 1450 psig at the inlet and 1650 psig at the discharge. The significant influence of high pressure oil seals on rotor system dynamics and stability is well documented in the literature. The purpose of this case history is not to repeat that

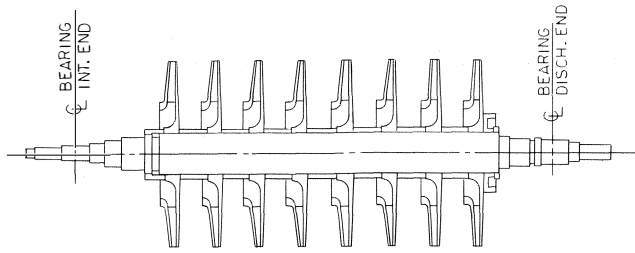


Figure 18. Eight-Stage HP Barrell Hydrogen Recycle Compressor Rotor.

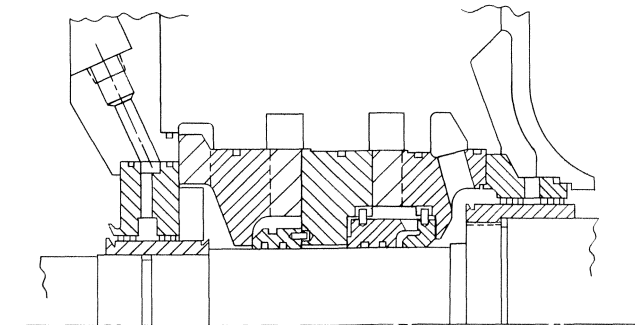


Figure 19. Multiple Breakdown High Pressure Floating-Ring Oil Seal.

theory, but rather to provide an example of the dramatic influence of oil seals on machine dynamics, particularly from an operations personnel perspective. With a basic understanding of how startup procedures influence oil seal forces, centering, and thus hydrodynamic coefficients and the resulting rotordynamics, operations people can easily employ a powerful technique in controlling high level nonsynchronous seal induced vibration. At the same time, unbalance-induced vibration can also be reduced to minimum levels. Elements of the problem and its solution included:

- specification of intermediate level suction pressure startup sequence for the turbine-compressor set in order to optimize unit vibration response-dynamics and stability of the compressor rotor.
- optimization of dynamic characteristics—amplification factor at the critical, frequency placement of the critical, damping capacity at the critical.
- optimization of stability characteristics—base log dec for normal operation, speed at onset of instability, system response to instability mechanisms.

Results of the Rotor Bearing System Dynamics Analysis

Undamped Critical Speed Analysis

As shown in Figure 20, compressor rotor undamped critical speed map, normal operating speed of 6000 rpm for this unit exhibits excellent separation margins for all potential rotor critical speeds:

- N_{c1} - first actual rotor critical speed
- N_{cr1} - first rigid rotor critical speed
- N_{c2} - second actual rotor critical speed
- N_{cr2} - second rigid rotor critical speed
- N_{ff1} - first free-free critical (third mode)

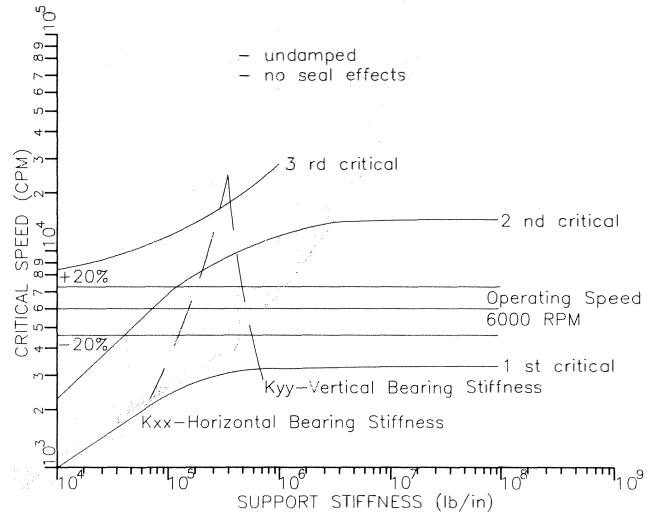


Figure 20. Recycle Compressor Undamped Critical Speed Map.

The compressor (rebuild configuration) exhibits a first actual rotor critical speed in the vicinity of:

$$N_{c1} = 3000 \text{ cpm}$$

from the undamped critical speed map, which does not account for the hydrodynamic interaction of the high pressure seals with the rotor-bearing system (Table 4). This effect is included in the more detailed confirming analysis, rotordynamic response to residual unbalance.

Table 4. Hydrodynamic Seal Characteristics—Recycle Compressor Optimization.

Design Parameter	Original Bearing Design	Optimized 5-Shoe Bearing Design	(Recommended) Optimized 3-Groove Bearing Design
K_{xx} (@ 4700 rpm)	827,000 lb/in	1,600,000 lb/in	410,000 lb/in
K_{yy} (@ 4700 rpm)	1,976,000 lb/in	2,800,000 lb/in	2,500,000 lb/in
C_{xx} (@ 4700 rpm)	1,878 lb-sec/in	3,390 lb-sec/in	743 lb-sec/in
C_{yy} (@ 4700 rpm)	5,327 lb-sec/in	5,190 lb-sec/in	5692 lb-sec/in
$\bar{K}_x = 2K_{Kxx}$ Kshaft	3.70	7.16	1.83
$\bar{K}_y = 2K_{Kyy}$ Kshaft	8.84	12.53	11.19
δ_u , Base Log Dec	+ .235	+ .146	+ .361
Unstable Frequency	1710 cpm	2130 cpm	1550 cpm
Non-Synchronous A. F.	13.4	21.5	8.74
1st Mode PRF(1)	1700 cpm	2100 cpm	1500 cpm
1st Mode PRF(2)	2200 cpm	2200 cpm	2200 cpm
2nd Mode PRF(1)	5000 cpm	5700 cpm	3800 cpm
2nd Mode PRF(2)	6250 cpm	6650 cpm	6150 cpm
A.F.-1PRF(1)	<< 13.0	<< 21.0	<< 8.0
A.F.-1PRF(2)	22.0	22.0	22.0
Amp @ Midspan	4.5 mils @ critical	4.25 mils @ critical	3.6 mils @ critical
S @ Midspan	100%	95%	80%
Amp @ Brg. #1	0.30 mils @ design	0.05 mils @ design	0.36 mils @ design
Amp @ Brg. #2	0.30 mils @ design	0.02 mils @ design	0.30 mils @ design
S @ Bearing (1)	100%	16%	120%
S @ Bearing (2)	100%	6%	100%

*A.F. = Amplification Factor

As is shown in the unbalance response analysis, no other rotor critical speeds are amplified below or above the compressor's normal operating speed range for speeds up to and exceeding 100 percent above the overspeed trip setting.

Rotordynamic Response to Residual Unbalance

The results are given in Figure 21 of the rotor unbalance response analysis for allowable unbalance, $U = 4 \text{ W/N oz-in}$ for the cases of:

- low suction pressure startup, $P_s = 100 \text{ psig}$.
- high suction pressure startup, $P_s = 800 \text{ psig}$.
- recommended startup suction pressure, which is a controlled intermediate suction pressure startup, $P_s = 400 \text{ psig}$, prior to increasing P_s .

The seal rings are actually floating bearing elements that, when locked, generate the full hydrodynamic fluid-film reaction. Seal lockup occurs on nonpressure balanced seal rings due to high radial friction loading at the seal ring-retainer interface. This lockup force is directly related to the seal pressure as the unit is brought online. The higher the seal pressure on unit startup, the greater the lockup position or eccentricity of the seal, and thus, the greater the destabilizing crosscoupled stiffness as well as beneficial direct-coupled damping generated. Optimization then requires a compromise between unbalance response and rotor stability.

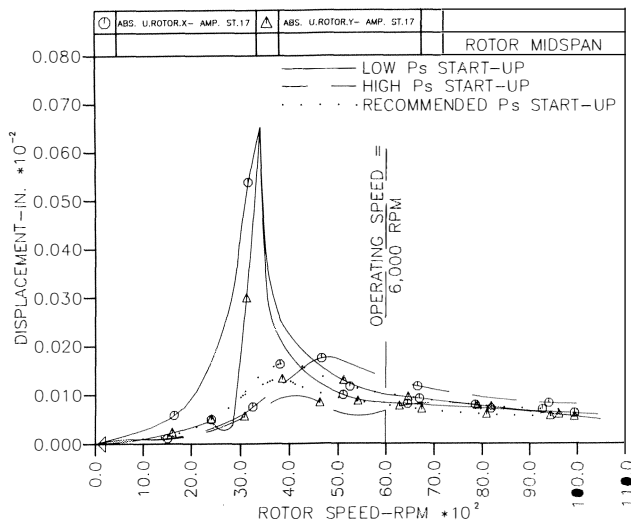


Figure 21. Rotor Unbalance Response Relative to Suction Pressure at Startup.

For the case of low suction pressure startup, the first critical speed is predicted to amplify at 3200 rpm to 3300 rpm, a highly amplified critical with poor damping characteristics.

For the case of high suction pressure startup, the first critical is predicted to amplify at 4200 rpm to 4800 rpm, a split critical with two discrete frequency vibration peaks which are well-damped in behavior.

For the case of the recommended startup suction pressure, the first critical is predicted to amplify at 3800 rpm to 4100 rpm, essentially a single peak response frequency with a well-damped envelope, and almost critically damped in behavior.

From the preceding discussion, it is clear that the specified suction pressure for startup of the turbine-compressor set will optimize the rotordynamics and vibration of the compressor rotor relative to the following:

- Amplification factor at the first critical
- Frequency placement of the first critical
- Damping capacity at the first critical

Rotor bearing system stability analysis also demonstrates that not only rotordynamic response, but stability as well, is op-

timized by the specified starting sequence with respect to compressor suction pressure, P_s , at startup.

Rotor Bearing System Stability

The results are given in Figure 22 of the compressor rotor-bearing system stability analysis for the following startup conditions:

- Low suction pressure startup, $P_s = 100 \text{ psig}$
- High suction pressure startup, $P_s = 800 \text{ psig}$
- Recommended startup sequence, intermediate $P_s = 400 \text{ psig}$

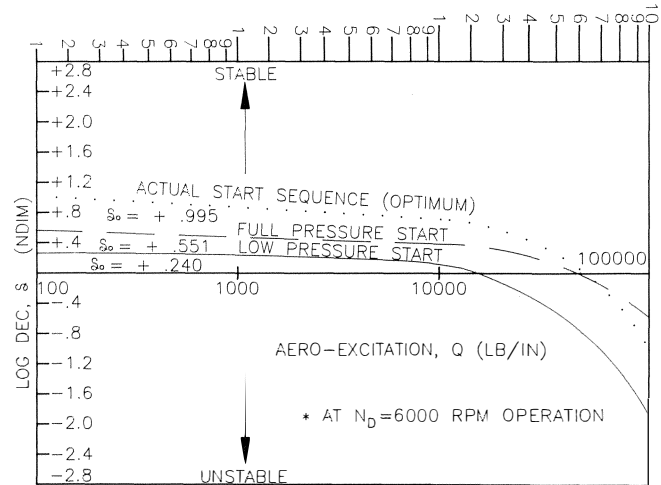


Figure 22. Rotor System Stability Relative to Startup Suction Pressure.

For $N = 6000 \text{ rpm}$ and $Q = 0 \text{ lb/in}$ (no aerodynamic excitation), the rotor-bearing stability analysis indicates the following values of base log dec, $\delta_o(\text{NDIM})$, for the respective cases:

- Low P_s Startup, $\delta_o = + 0.240$
- High P_s Startup, $\delta_o = + 0.551$
- Recommended P_s Startup, $\delta_o = + 0.995$

For $N = 6000 \text{ rpm}$ and $(\log \text{dec}) = 0$, the level of aerodynamic cross-coupling, Q , required to exceed the threshold of instability is respectively:

- Low P_s startup, $Q = 15,500 \text{ lb/in}$
- High P_s startup, $Q = 26,000 \text{ lb/in}$
- Recommended P_s startup, $Q = 30,000 \text{ lb/in}$

From these results, it is clear that the recommended suction pressure for startup of the turbine-compressor set will optimize the rotor-bearing-seal system stability of the compressor rotor.

Conclusions

- The recommended starting sequence for the turbine-compressor set relative to compressor suction pressure will optimize the rotordynamics (vibration and stability) of the compressor rotor.
- Startup mode will optimize the following rotor vibration characteristics:
 - amplification factor at the first critical
 - frequency placement of the first critical
 - damping capacity at the first critical
- Startup mode will optimize the following rotor stability characteristics:
 - base log dec, δ_o , for normal operation
 - speed at onset of threshold of instability
 - overall system resistance to aeroexcitation

- The compressor rotor's first critical speed is predicted to amplify at:

$$N_{c1} = 3800 \text{ rpm to } 4100 \text{ rpm}$$

essentially a single peak response frequency with a nearly critically damped envelope, for specified startup conditions.

- The compressor rotor's overall system stability indicates a base log dec of

$$\delta_o = + 0.995$$

for $N = 6000 \text{ rpm}$ operation with $Q = 0 \text{ lb/in}$ (no aerodynamic loading), a highly stable configuration, for specified startup conditions.

CASE STUDY 5

Redesign of Rotor Fits and Retainer Rings for A NO_x Module Rotor to Stabilize Rotor Build and Detune Blade Resonance

Problem Definition

The low pressure expander rotor (Figure 23) of this NO_x installation dealt the user many and varied problems from the very start of its operation. These included problems with performance, blade resonance, unit vibration during process transients, and most notably rotor upsets during unavoidable and frequent overspeed and overtemperature excursions and tripping off line due to upstream process upsets. These offline trips resulted in the rotor decel down through the critical experiencing high vibration levels. Any attempt to restart after such an excursion resulted in an extremely rough running rotor. Upon disassembly, the rotor was found to have high runouts due to rotor fits and retainer rings allowing the overhung high temperature expander rotor to become skewed and then take a permanent eccentric set on the shaft. Each trip necessitated rotor disassembly in order to relieve the fit runouts and straighten the rotor build. Elements of the problem and its solution included:

- verification that lateral rotordynamic behavior of the unit was acceptable and not the cause of the problem.
- demonstration through finite element analysis that the thermal and centrifugal growths of the rotor retainers were unacceptably high, allowing the rotor to shift and take a permanent set.
- redesign of rotor retainers and fits to stabilize the rotor.
- explanation of severe fretting of blade tips of two-piece expander rotor due to loss of fit of old retainers allowing the rotor's fundamental in-phase torsional resonance to drop and become

coincident with the blade natural frequency (as measured by testing). Redesign of the rotor fits raised the rotor torsional critical speed and detuned it from the known blade resonance.

Results of the Rotor Bearing System Dynamics Analysis

The overall rotordynamic behavior of the NO_x module on accel to running speed and during normal operation at design point was found to be completely acceptable relative to machine critical speeds, unbalance response, and stability.

Undamped Critical Speed Analysis

The undamped critical speed map for the NO_x rotor indicates excellent operating margins relative to normal operating speed and all machine critical speeds (exceeds API margins).

The analysis indicates rigid rotor modes with little bending, good damping, and moderately lightly loaded bearings.

Relative to the observed failure mode of the rotor, shaft end flexibility is not found to be a problem, as is evidenced by dynamic rotor mode shapes in the load (Y) and no-load (X) directions.

The rotor critical speeds are demonstrated not to be sensitive to the potential loss of fit of the expander rotor (and compressor rotor) on the shaft. As such, loss of fits adversely affects the rotor mechanically, but does not shift its critical speeds.

Rotordynamic Response to Residual Unbalance

The unbalance response analysis confirms the critical speed analysis in that the normal speed range of the NO_x rotor, including up to trip speed, is free of rotor critical speeds for both a rotor with good mechanical integrity and for a rotor with loss of good fits.

Split, well-damped conical rotor modes exist all the way from 500 rpm to approximately 6500 rpm, mainly due to high bearing stiffness asymmetry. These rigid rotor components are well-damped as is evidenced by:

- low amplification factors.
- gentle phase shifting on startup.

Third mode response occurs at 14,000 rpm to 15,000 rpm, well above even the trip level of the rotor, and is itself very well damped for a rotor's third bending critical.

Rotor Bearing System Stability

The rotor bearing system stability analysis of the NO_x rotor confirms a highly stable rotor bearing design configuration up through and above 10,000 rpm rotor speed.

The base logarithmic decrement (log dec) of the expander rotor is $\delta_o = + 0.810$, and the base log dec of the compressor rotor is $\delta_o = + 1.280$, indicating a highly stable rotordynamics design.

Even for highly elevated levels of aerodynamic excitation or fluid dynamic jolting, the NO_x rotor is not expected to experience rotor-bearing instability at the extreme conditions of overspeed trip, overtemperature trip conditions, and high radial vibration.

Rotor Torsional Critical Speed Analysis

A detailed rotor torsional natural frequency analysis of the NO_x module yields the following results (Figure 24):

- rotor fundamental out-of-phase mode $-f = 6058 \text{ cpm}$
- rotor fundamental in-phase mode $-f = 22,162 \text{ cpm}$

These torsional modes do not coincide with any potential rotational excitation frequency.

However, the in-phase mode does coincide almost exactly with the exducer section blade natural frequency of the two-piece expander wheel as measured and reported from the NO_x module rotor bump test which was performed earlier.

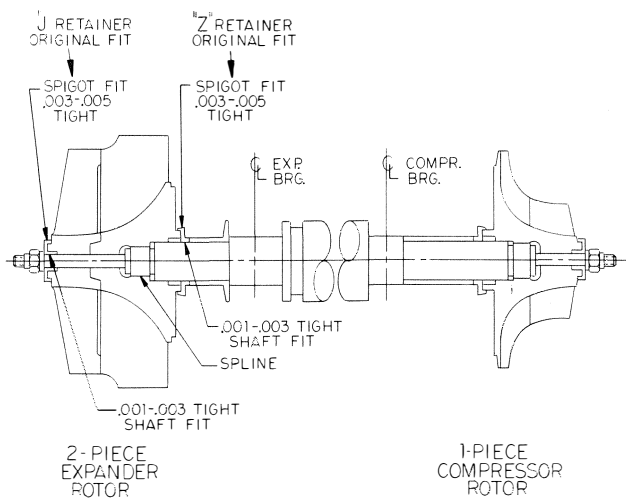


Figure 23. 5,500 HP Low Pressure Stage NO_x Module Rotor.

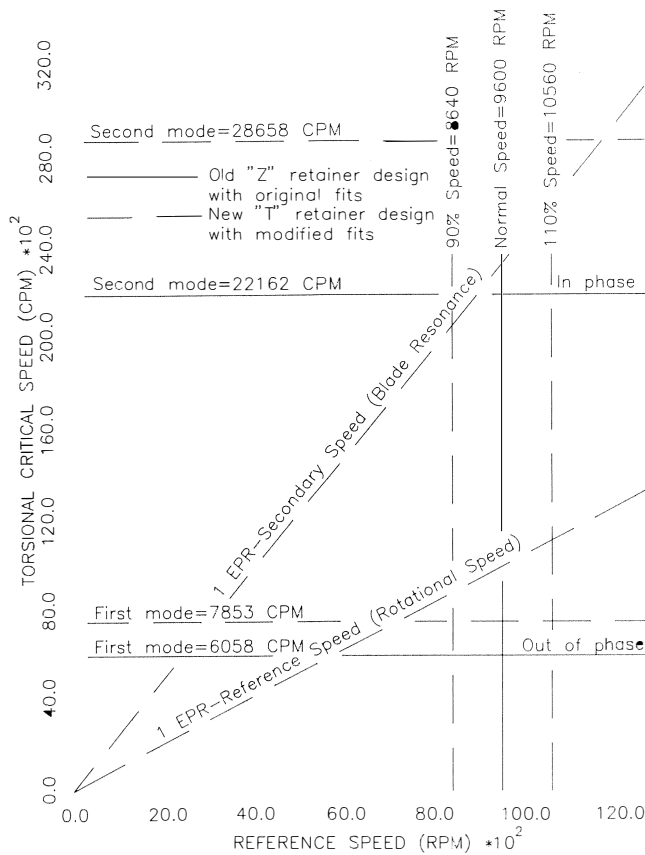


Figure 24. Rotor Torsional Critical Speeds for Existing and Redesigned Retainers.

The inphase rotor mode shape places both expander rotor and compressor rotor fit attachments precisely at the nodal points of the two-node mode, the worst case scenario for imparting maximum vibratory torque at resonance, as discussed by Mondy and Mirro [3], into the expander rotor, which could subsequently excite the exducer blade resonance leading to severe fretting.

The torsional analysis was based on an assumed loss of fit of the expander rotor retainers (principally, main rear "Z"-retainer), thereby allowing for additional torsional flexibility of the shaft and thus dropping the in-phase resonance to 22,162 cpm, coincident with the blade natural frequency.

Reanalysis of the rotor torsional vibration response without loss of fits on the rotor retainers results in the in-phase resonance shifting upwards in frequency to 28,658 cpm, no longer coincident with the exducer blade natural frequency.

Analysis thus reveals that not only will proper rotor fits provide acceptable separation margins between rotational frequencies, rotor torsional natural frequencies and blade flatwise natural frequencies, and improving if not solving the problem of severe blade fretting between the two expander rotor halves, but may also solve the problem of rotor fit loss and the resulting unstable rotor build.

Stress and Deflection Analysis of NO_x Expander Rotor, Retainers, and Fits

In the initial work done on the expander rotor, it was concluded that the distress experienced by the NO_x module during overspeed trip was caused by the fact that the retainers malfunctioned, i. e. did not provide an adequate fit between the expander wheel and the shaft. Because the coefficient of thermal expansion of the disk is at least 35 percent greater than that of

the retainers or of the shaft, it appeared doubtful that the retainer could maintain good contact with the shaft while restraining the wheel rear fit from substantial radial thermal and centrifugal growth.

The sequence of events leading to "kinking" of the shaft is not quite clear, however, it was calculated that it takes only about 110 lb of lateral load to deflect the shaft end 0.004 in, the measured runout at disassembly. A possible explanation was that the overspeed and overtemperature excursions were severe enough to create sufficient wheel looseness and dynamic unbalance to cause it to experience a high vibration from trip down through the critical. In this event, "cocking" of the retainers apparently occurred with their subsequent tightening during coastdown and cool-down.

Analysis of Rear "Z"-Retainers and Rotor Fits

The thermal coefficient of the A-286 expander rotor is about 35 percent higher than the 15-5 Ph shaft and 17-4 Ph retainers.

This differential thermal growth results in additional radial interference at the rear retainer outside fit of 0.005-0.006in, resulting in a net retainer hoop stress of $\sigma_z = 53,000$ psi, without including centrifugal growth.

The actual growth at the bore of the expander rotor at the rear retainer at speed and temperature is:

~ 0.005 in radial due to thermal growth.

~ 0.005 in radial due to centrifugal growth.

Thus, the cumulative potential loss of fit is about 0.010 in radial or 0.020 in on the diameter.

The rotor maximum hoop stresses are acceptable with σ_z (max) ~ 42,000 psi.

The principal problem with the existing "Z" retainer design (Figure 23) is inadequate length of fit, resulting in gross retainer deflection at the shaft fit and the loss of fit.

With this much thermal and centrifugal hub growth, it would not be feasible to stabilize the expander rotor with a simple inside fit, i. e., bushing the rotor bore and interference fitting the shaft. This would result in very heavy fits, difficult to assemble, and probably extremely difficult if not impossible to disassemble.

An outside fit design is required with a sufficiently long retainer length in order to minimize retainer deflection at the actual retainer to shaft controlling shrink fit, thereby retaining a good fit in operation.

The possible option of an integral rear retainer/seal runner/thrust collar is not feasible, since it would require major manufacture in the area of designing a new split seal housing and split seal rings, in order to assemble the machine. Even so, this may not be feasible due to the way this module is assembled.

The only reasonable design alternative, short of expensive (and maybe exotic) redesign, is to counter bore the rear rotor hub deeper axially and extend the retainer ring inside the counterbore of the rotor.

Redesign of Rotor Retainers of Rotor Fits

Details of the rear retainer ring re-design follow (Figure 25):

- "T"-design has a maximum possible axial length along the shaft.
- the major (controlling) fit (inside counterbore) is a fairly heavy shrink fit at 0.006 in \pm 0.001 in tight diametral (originally 0.002 in \pm 0.001 in tight).
- the major fit length should be approximately 2 \times spigot depth ~ 1.620 in.
- the minor fit to the shaft should be a sliding pilot fit so it cannot seize the shaft, 0.001 in \pm 0.001 in tight diametral.
- the center is relieved between fits.

- the outside fit (spigot) is 0.001 in \pm 0.001 in tight diametral (originally 0.004 in \pm 0.001 in tight). This will grow approximately 0.010 in tight at normal operating conditions.
- the spigot thickness (retainer to hub) ideally approaches a ratio of 1:1 for optimum compatibility of stress and deflection.
- the material remains 17-4 ph.
- any possible added vertical thickness is desirable, without modification to the rotor.
- the maximum possible sleeve thickness is retained.

The redesigned rear retainer provides a total radial compressive load of approximately 133,000 lb on the shaft at steady-state operation of 9600 rpm and 600°F (Figure 26). This is an improvement of a factor of 5.5 over the existing retainer design. The total force between the wheel and retainer was also increased by almost 30 percent. These improvements provide enough restraint even during a process upset when a sudden temperature increase does momentarily heat the wheel, causing it to grow an additional amount relative to the shaft, and coincident with an overspeed trip.

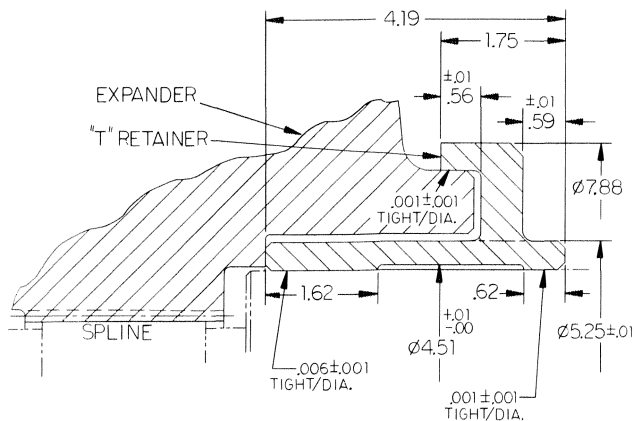


Figure 25. Redesigned "T-Section" Main Rear Rotor Retainer Ring.

The additional machining (counterbore) at the rear of the expander wheel creates a negligible increase (less than one percent) in effective (vonMises) stress at steady-state operation.

Nose Pilot Retainer Fit Modifications

The nose pilot retainer keeps the existing "J"-design, but the fits have been modified (Figure 23).

The inside fit, retainer bore to shaft, is modified to 0.000 in \pm 0.001 in line-to-line diametral (originally 0.002 in \pm 0.001 in tight).

The outside fit (spigot) is also modified to 0.000 in \pm 0.001 in line-to-line diametral (originally 0.004 in \pm 0.001 in tight). This will grow 0.002 in to 0.003 in tight at speed and temperature.

Unlike the original design which, with its tighter nose pilot fits allowed the rotor, once kinked, to take a permanent set due to front and rear controlling fits, with this differential fit scheme, the rear retainer being the primary controlling fit and the nose retainer being the pilotting slip fit, the rotor will not be able to take a permanent set holding the expander stage nonconcentric. The axial holding force will then locate the nose fit, the recommended prestretch being 0.006 in.

Conclusions

- The expander rotor rear retainer is the primary and controlling fit. It has been modified from a "Z" to an "inverted T" design as shown in Figure 25. The controlling fit, pilot fits, and spigot

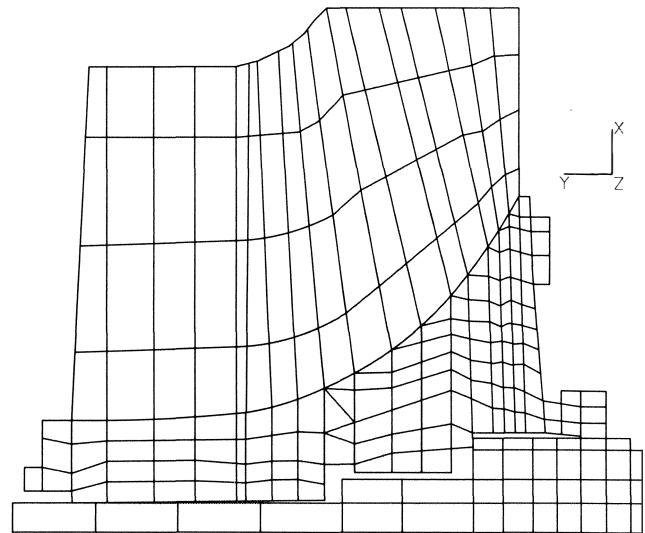


Figure 26. Finite Element Deformed Shape of Expander Rotor and Redesigned Rear Retainer at Speed and Temperature.

fits are as indicated. The new design provides sufficient restraint for the rotor even during process upsets.

- The nose pilot retainer keeps the existing "J"-design, but the fits have been modified. The redesigned differential fit arrangement minimizes the tendency of the rotor to become permanently skewed on the shaft.

- The redesigned rotor retainers and fits will keep the rotor stabilized at speed and temperature and will serve to detune the rotor's in-phase torsional resonance, thereby uncoupling it from the excuder blade fundamental natural frequency at 22,162 CPM, and raising it to 28,658 cpm. This redesign should alleviate, if not eliminate, the severe blade fretting problem on the two-piece expander rotor.

- For the two-piece expander rotor with interference fit blade halves or "blade tip dampeners," additional restoration/reclamation recommendations were followed including optimization of blade contact remachining angles, utilization of a high-temperature antifretting blade-tip coating, and an improved hub fit design at the bore of the two expander rotor halves, improving rotor mechanical integrity.

- Several secondary recommendations included reorientation of the tilting-pad journal bearings to a load-between-pads configuration, reduction of the operating journal bearing clearances, and elimination of dynamic unbalance from the rotor, in an effort to optimize machine dynamics.

- Redesign of the unit and subsequent restart were successful and operation continued until an unrelated problem forced unit shutdown. An unexpected process upset coincided with shutdown, driving the unit into its most violent offline trip recorded to date. Subsequent inspection found the rotor build remained stabilized through this excursion, with no indication of loss of fits during the transient and no residual rotor runouts.

CASE STUDY 6

Troublesome Nitric Acid Trains Are Successfully Retrofit with Optimized Radial Bearing Inserts

Problem Definition

A recurring problem has been nitric acid expander and compressor rotors (Figure 27), which have been running for some time and are experiencing a significant degradation in time relative to both synchronous and nonsynchronous vibration levels.

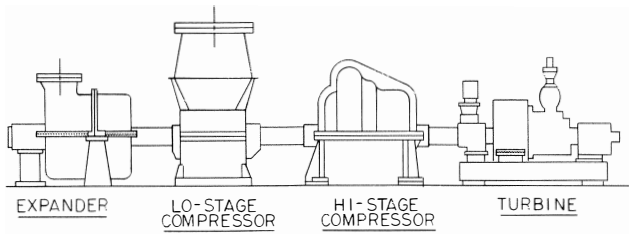


Figure 27. Nitric Acid Train General Arrangement.

Very high vibration levels have in some instances led to the installation of aftermarket bearing designs—often worsening the problem. Coupled with maintenance-related problems, the overall problem can be compounded and result in great losses due to forced downtime and major plant outages. Elements of the problem and its solution included:

- rotor system dynamics and stability analysis point out the inherent bearing instability which is typical of many of these units, which is somewhat insensitive to the specific output of the unit (or its size).
- stabilized bearing insert design is retrofitted with great success in each case.
- previously installed aftermarket bearing designs were substandard in terms of generally accepted standards of hydrodynamic bearing design and the machinery suffered accordingly high vibration, machine damage, and in some cases, severe damage to the bearings.
- correction of existing problems such as loose bearing housings.

Results of the Rotor Bearing System Dynamics Analysis

The lateral analysis of the subject nitric acid train hot gas expander rotor (Figure 28) indicates well behaved rotordynamic response with operation near 9000 rpm well above the first rotor critical at 3000 rpm (Figure 29). This resonant peak is a well-damped bearing critical, a bouncing or cylindrical mode, which is of no concern as a synchronous vibration component. The first mode rigid bearing critical is above 13,500 rpm allowing the expander to operate as a rigid rotor over its range of operation.

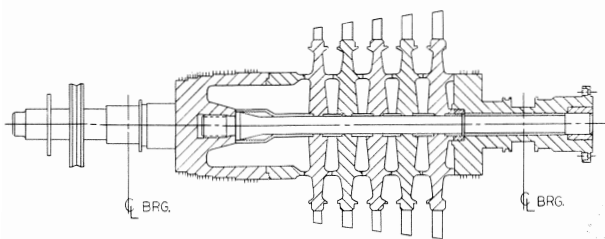


Figure 28. 10,000 HP Nitric Acid Hot Gas Expander Rotor.

The high critical speed ratio, operating speed/critical speed = 3.0, is not so fortuitous for the unit relative to nonsynchronous re-excitation of the balance resonance as an instability mechanism. For this class of nitric acid expanders, the mechanism which drives the rotor instability is the classical light load bearing instability which results from high-speed oil whirl. The original units are highly susceptible to this instability mechanism as they operate on plain sleeve bearings. The existing design of the rotor-bearing system for these expanders has been analyzed for stability. The result is a log dec of $\delta = -0.25$, a highly unstable configuration. This analysis result is confirmed by recurring operating problems experienced by many users relative to high

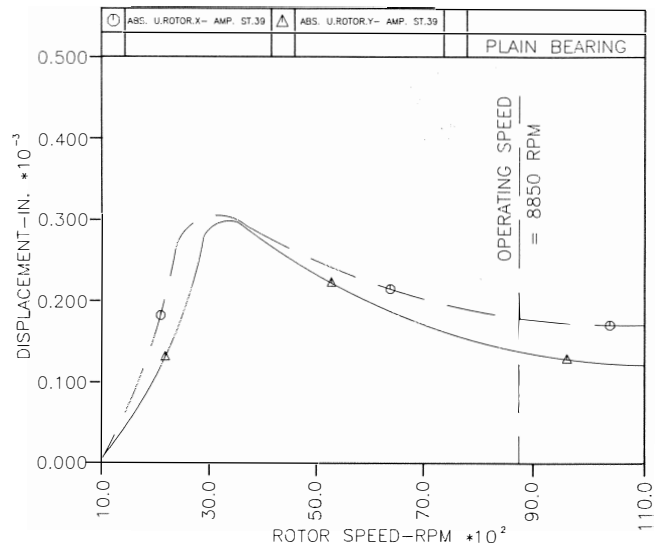


Figure 29. Nitric Acid Expander Rotor Unbalance Response.

level subsynchronous vibration problems experienced on their units (Figure 30).

Operating Experience

For the general machine population in this machinery class, many units of which have been in operation for more than 10 years, a very high incidence rate exists for this rotor instability problem. Some units showed early symptoms of rotor instability in the form of low level subsynchronous vibration, while for others it did not show up in the vibration signature until later in operation. The instability problem appears and then worsens as the unit gradually degrades from the as-new condition, since

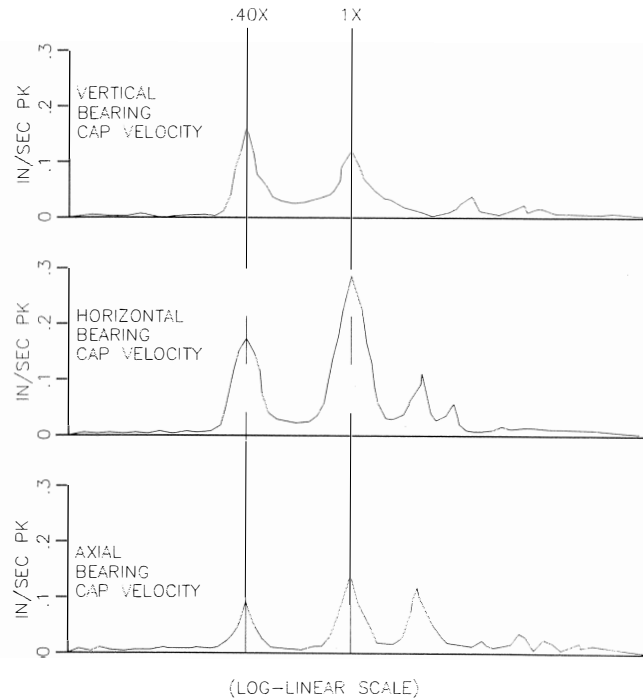


Figure 30. Expander Tri-Axis Bearing Cap Velocity Vibration Spectrum.

this particular machine instability is very temperamental and depends to a large extent on small variations in operating conditions such as speed, load, ambient conditions, lube oil temperature or pressure, bearing wear, or degradation, etc.

Experience indicates that many bearing retrofits have been made by users who have struggled with this instability problem in past years. Unfortunately, many of these retrofit bearing designs supplied by aftermarket sources have been found to be substandard in terms of generally accepted standards of hydrodynamic bearing design. As a result, these retrofits not only did not provide a bearing design capable of stabilizing the rotor system, but worse, in some instances degraded the system even further through improper design resulting in loss of load capacity or hydrodynamic damping. The end result was continuing vibration problems, bearing damage, and in some cases further machine damage.

Stabilized Bearing Design

An optimized multiple pressure dam bearing insert design (Figure 31) resulted from analysis of the rotor system instability problem. This bearing redesign stabilizes the rotor, has been shown analytically to be the optimum solution, and has been used in numerous retrofits with 100 percent success in eliminating all subsynchronous vibration as well as improving upon synchronous levels. Instability threshold speeds have been elevated from near operating speed to 100 percent above operating speed. The log dec has been improved from $\delta = -0.25$ to $\delta = +0.30$ for the rotor system.

Conclusions

- Rotor-system dynamics and stability analysis point out the inherent bearing instability which is typical of many of these expander units.
- Previously installed aftermarket bearing designs were not capable of stabilizing the rotor system and were substandard in terms of generally accepted standards of hydrodynamic bearing design.
- Correction of existing problems such as loose bearing housings was necessary on many of the older units, greatly reducing operating vibration levels.
- A stabilized multidam bearing insert design was retrofit with great success in every case.

CASE STUDY 7

Large Induction Motor/Integral Gear Compressor Experience High Level

Torque/Current Pulsations Preventing Unit Startup

Problem Definition

This installation is at an air separation plant near Milan, Italy, and the problem reached crisis proportions as the unit experienced violent pulsations approximately 35 seconds into the normal startup cycle during multiple attempts to restart. Resulting high level radial vibration readings were observed at the same time approaching 10 mils on some probes and a very loud "thudding" could be heard synchronized with the pulsations. The following machine signatures were provided for the transient condition: polyphase current oscillograms, active power, motor speed, and radial vibration spectrums. Elements of the problem and its solution included:

- determination that the problem was more likely electrically induced rather than a flow induced load instability being followed by the motor.
- looking at the starting cycle, it was determined that the rotor circuits were balanced during the acceleration up to the point where the slip rings were shorted out.

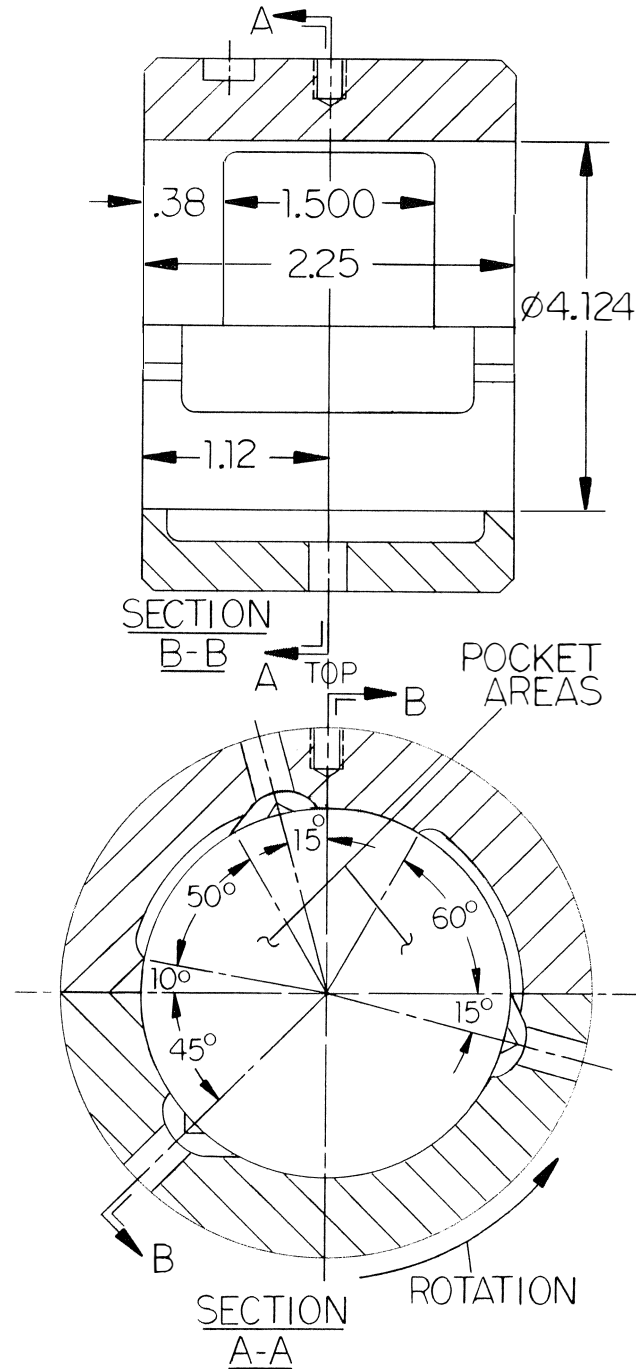


Figure 31. Redesign Multiple Pressure-Dam Bearing.

- eighteen seconds after the rings are short circuited, current oscillations occur at double slip frequency with a strong harmonic component, indicating one phase of the power supply is open, the contactor between two rings failed to close, or had an otherwise open circuit.
- recommendation to test the starting circuitry, and not the motor circuit, for the open phase and correct it. This was followed by the motor manufacturer removing the motor from the plant, returning it to the factory, undergoing extensive testing, and a final determination being made that a burned phase existed in the starting circuitry. Correction, reinstallation and subsequent startup resulted in successful operation.

Initial Analysis Based on Initial Data

For a motor rotor, a rotating magnetic, electrical, or mechanical asymmetry are the causes of many major motor vibration problems. These are caused by a bent shaft, non-circular rotor build, or defective or broken rotor bars. The frequency of vibrations resulting from motor asymmetry are always multiples of electrical or rotational frequency. These components are not present in the site test data (Figure 32). The motor is possibly responding to a cyclic load being imposed upon it.

It is significant to note that for a wound-rotor motor (slip-ring) induction machine such as this, one does not have an exact means of speed control under varying load conditions (pulses). That is, a given point on the controller will not necessarily assure a given speed. For a given secondary resistor value, the speed can vary (or pulse) widely if load torque, voltage, or other conditions vary. This would then result in a cyclic current draw and active power generation, Kw.

The data does suggest a possible flow induced pulsation problem giving rise to high vibration and high motor operating transients. This possibility is supported by the 90 cpm low frequency component on the bull gear and second stage rotor (Figures 33, 34). It was determined, however, upon assessment of the compressor flow condition, that the unit was not being operated in surge. Also, installation of pressure transducers in the associated piping of all four compressor stages resulted in no indications of induced flow pulsations.

Another motor problem possibility is with the rotating magnetic pull of the wound rotor, which could possibly give rise to low frequency harmonic excitation. This would typically manifest itself as a torsional oscillation, which in a system such as this integral gear compressor, could easily be translated into a radial and axial vibration. This possible excitation of the rotating magnetic field is due to the electrical spring constant, K, and a constant, H, which is a measure of relative system inertias. Estimating the large compressor inertia to be about 4X motor inertia, then

$$f = 2.2(K/H)^{1/2} = 2.2(1/4)^{1/2} \sim 1.1 \text{ Hz.}$$

This is close to the problem frequency indicated.

Although many other possible problem areas exist, the most likely possibility was considered unbalanced rotor circuits. This could result in $2 \times$ slip frequency torque pulsation, modulated by $1 \times$ slip frequency. This is consistent with the observed vibration frequency and its corresponding beat pulsation frequency:

- Vibration frequency = 90 cpm
- Beat frequency = 45 cpm = 0.75 Hz = 1.5 percent slip

Since slip is approximately proportional to torque, or load, slip frequency increases when load increases. This correlates with the motor data for the cases of inlet guide valve (IGV) five degrees opened and ten degrees opened. Thus, the beat frequency could be slip frequency.

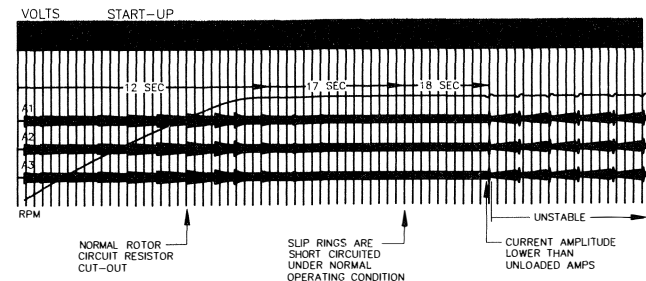


Figure 32. 10,000 HP Induction Motor Starting Cycle Transients.

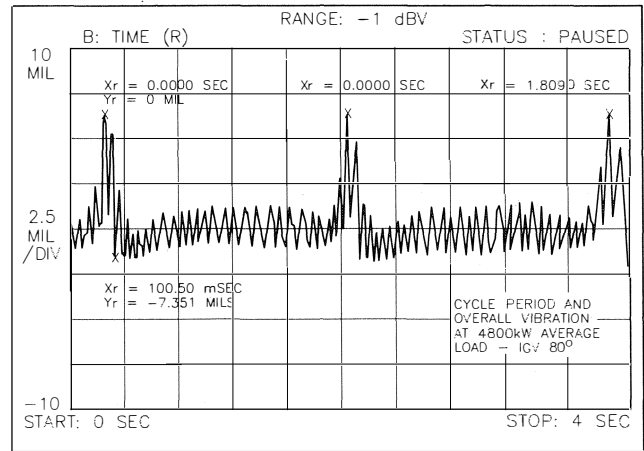


Figure 33. Time Base Cyclis Vibration of the Integral Gear Compressor Bull Gear.

An initial check was proposed prior to in depth motor testing in order to determine if the problem was in the external switching circuitry, possibly one of the three-pole contactors was not closing (for example, if the leads burned off), leaving a motor circuit open. Or possibly a mechanical malfunction occurred in the poles in the switch. This, then could result in the observed rotor electrical unbalance and subsequent twice slip frequency torque pulsation modulated by slip frequency.

Final Analysis Based on Final Data

Examination of the current oscillograms for the full starting cycle (Figure 32) shows that rotor circuits were balanced during the acceleration up to where the slip rings were shorted out (no oscillation of current).

The observed stepup occurs each time a section of the resistor in the rotor circuit is cut out. In one second, the current drops off as the speed increases. This is as expected.

Approximately 18 seconds after the rings are short circuited, the current are seen oscillations at double slip frequency with a strong harmonic component. This fits exactly with the expected performance if one phase is open. the contactor between two rings fails to close, or has an open in its circuit. If the open was in the motor circuit, then this type of pulsation would have occurred throughout the starting cycle.

The severe swing in current, and resulting torque, are due to the high reactance (approaching magnetizing reactance) when the flux in the motor lines up with this open rotor phase (line to line).

The only other possible explanation is that a rotor phase burned open almost simultaneously with the contactor closing that shorts the rings. This would very likely have ended up in a short circuit, which it did not.

A test for the phase balance of the rotor circuits (with stator short circuited) proved the motor stable.

If one contactor pole failed to close, it should be possible to check the continuity of the circuit. A contactor pole might fail once, and then appear all right, but it might fail again, or consecutively.

If it is a lead burned open, the open circuit is probably at a brazed or soldered connection. It may require a meter reading low circuit resistances to detect the unbalance and locate the spot.

The harmonics of the double slip frequency are caused by the oscillation of the speed and angle. The flux which is trapped by the shorted rotor winding swings in angle causing a higher frequency component of current. The current, which is due to an

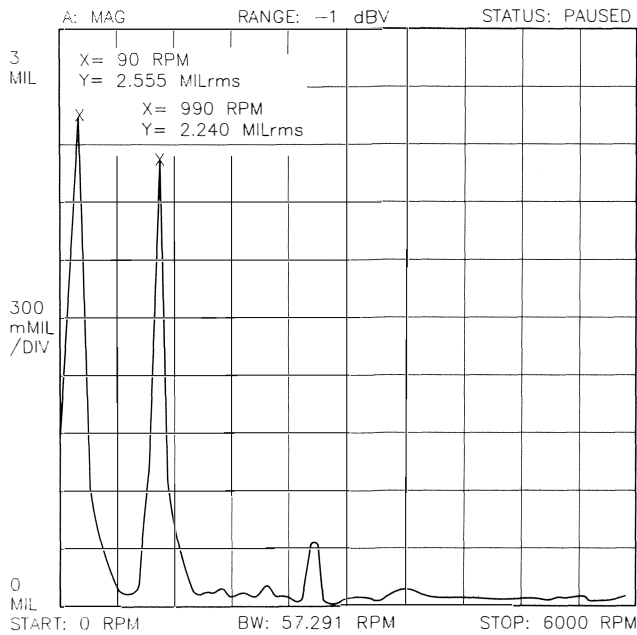


Figure 34. Vibration Spectrum of the Integral Gear Compressor Bull Gear.

average plus an oscillating component, may actually dip below the no load current, as is shown on the oscillogram.

Problem Resolution

As a result of the analysis, a recommendation was made to test the starting circuitry, and not the motor circuit, for the open phase and correct it. This was followed by the motor manufacturer removing the motor from the plant, returning it to the factory, undergoing extensive testing, and a final determination being made that a burned phase existed in the starting circuitry. Correction, reinstallation, and subsequent startup resulted in successful operation.

Conclusions

- A determination was made that the problem was electrically induced and not a flow induced load instability.
- The startup data indicates that the rotor circuits were balanced during the acceleration up to the point where the slip rings were shorted out.
- After the slip rings were short circuited, current oscillations occurred at double slip frequency with a strong harmonic component, indicating one phase of the power supply was open.
- A final determination was made that a burned phase existed in the starting circuitry. Correction, reinstallation, and subsequent startup resulted in successful operation.

CASE STUDY 8

Compressor Rerate Analysis Demonstrates that Plain Sleeve Bearings, Not a Tilting Pad "Upgrade," Are Optimum for Unit Dynamics and Stability

Problem Definition

This propylene compressor (Figure 35) was being performance rerated and the complete unit rebuild was to include a mechanical upgrade by retrofitting the existing journal bearings with an optimized design. A strong desire was expressed by the client to retrofit with a five-tilting shoe design, considered the obvious best replacement bearing for a machine upgrade. However, the results of this analysis show this large centrifugal compressor to be a classic example of a common occurrence not well

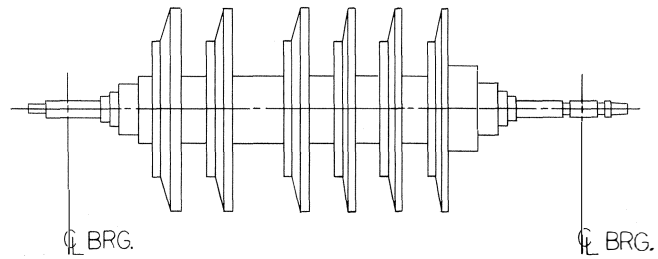


Figure 35. Six-Stage 13,000 HP Propylene Compressor.

understood in rotating machinery applications—that for many machines the specification of tilting-pad journal bearings is one of the least desirable choices from the standpoint of improved mechanical performance. Elements of the problem and its solution included:

- analytical results clearly demonstrated that even optimum tilting-pad bearings optimized in terms of length/diameter ratio, clearance, preload, etc., generated unacceptably high film stiffness for the compressor rotor, resulting in node points at the bearings. This condition resulted in unacceptable mechanical performance both at normal operating speed and in the critical, which was traversed with a very high amplification factor, $AF = 22$.
- an optimized three-axial groove plain insert bearing design is shown to demonstrate superior dynamics and stability characteristics over a wide range of manufacturing tolerances, and is considered the bearing of choice for this application by analysis and from past practical experience with this class of machinery.
- startup and operation on the redesigned bearings has been highly successful, the rotor operating with very low vibration levels and running smoother than it ever ran before the rework.

Results of the Rotor

Bearing System Dynamics Analysis

A detailed rotor system dynamics analysis and bearing design optimization study had been performed in support of a compressor rerate for a six-stage rotor rebuild. The propylene refrigeration unit operates at approximately 13,000 hp .007 4700 rpm.

A comprehensive analysis was made after having developed analytic rotor models which account for shear deformation and include general linearized gyroscopics. Fluid film bearing hydrodynamic characteristics were obtained using the latest finite element analysis techniques to analyze the dynamic lubricant film. Once having established detailed dynamic system models, rotordynamics studies were performed.

The results of the analysis can be summarized as follows. Rotor critical speeds occur at:

$$N_{c1} = 2200 \text{ rpm}$$

$$N_{c2} = 6200 \text{ rpm}$$

with the first critical being a highly amplified pure rotor bending mode with an AF , amplification factor = 22 (synchronous).

Bearing design optimization studies confirmed that an optimized plain insert bearing design is not only the best suited radial bearing for this application, but that a segmented tilting-shoe bearing would be a gross misapplication of that very common bearing "upgrade." This conclusion results from the fact that optimized five-tilting shoe bearings, at both the critical speed and design speed, generate too much film stiffness resulting in node points at the bearings for this particular application. This, in turn, results in unacceptable dynamic characteristics for the rotor.

The rotor with new optimized plain insert type journal bearings demonstrates superior mechanical performance relative to tilt-pad designs, as well as significant improvement over the existing 3 multilobe bearing design in terms of dynamics, stability, and reliability.

Undamped Critical Speed Analysis

The first critical for the compressor is traversed as a rigid bearing critical (Y-direction stiffness), $f_1 = 2200$ cpm, with the associated high amplification factor for the first pure bending mode. First critical is 47 percent of design speed.

The horizontal component of the second critical is critically damped, making the actual (vertical component) second critical speed occur at about $f_2 = 6250$ cpm, which is 33 percent above design speed.

The first free-free bending mode (third mode) occurs at about 4800 cpm, near running speed, but is not of interest since the high journal loading prevents operation at extremely low bearing stiffness.

It is evident that no API separation margin problems exist in the present engineering study.

Dynamic Response to Rotor Unbalance

The results of the rotor response analysis are given in Figure 36 for the unit for unbalance = 4 W/N oz-in.

The first peak response frequency (1PRF) is shown to occur at approximately 2200 rpm with a well-damped split component occurring at approximately 1700 rpm. The first critical, $f_1 = 2200$ rpm, is highly amplified, $AF = 22$, as can be seen at rotor midspan.

The second peak response frequency (2PRF) is seen at approximately 6250 rpm with a critically damped split component occurring at approximately 5000 rpm.

The rotor response studies are done for an unbalance level of $U = 4W/N$ oz-in and applied in a general modal unbalance distribution across the rotor in order to amplify all rotor modes. This is shown to result in midspan response at the first critical of 1.5 mils, or $3 \times 1.5 = 4.5$ mils for the unbalance defined in API Std. 617, para. 2.8.1.9 [4].

Running speed amplitudes at the bearings show reasonable levels at 0.1 mils (or $3 \times 0.1 = 0.3$ mils) as compared with midspan and overhangs in the dynamic mode shape, indicating

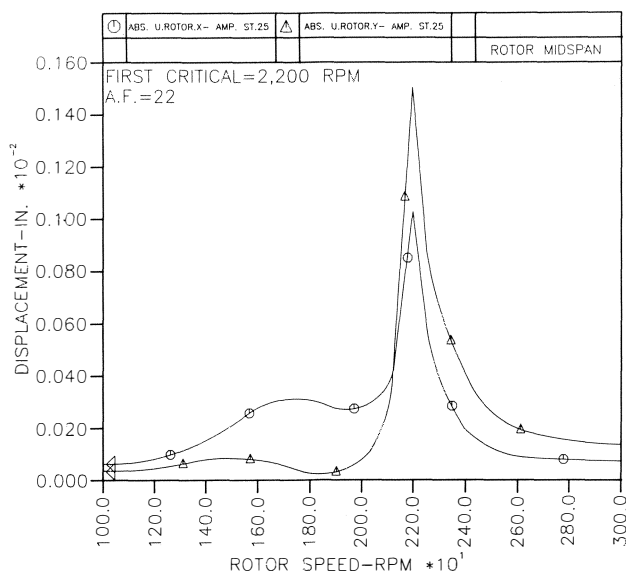


Figure 36. Rotor Unbalance Response of the Propylene Compressor.

the bearings are not approaching node points for the existing insert bearing design.

Rotor bearing System Stability

The rotor-bearing stability analysis indicates a base log dec, $\delta_o = + 0.235$ ($N = 4700$ rpm, no aeroexcitation) for the existing three lobe insert bearings.

A finite stability threshold does exist for the existing bearing design at about 8900 rpm for the case of no aerodynamic loading. This instability speed could be degraded with the effects of:

- aerodynamic excitation, K_{xy} , on the rotor.
- manufacturing tolerances on the bearings.
- bearing clearance variations.

The oil seals do not generate significant hydrodynamic forces to alter the rotor's dynamic behavior for the low pressure application of the propylene compressor.

Bearing Design Optimization Study

Various bearing designs were considered for the present application:

- five-tilting pad, 50 percent preload
- five-tilting pad, 30 percent preload
- five-tilting pad, 0 percent preload
- four-tilting pad, 50 percent preload
- four-tilting pad, 0 percent preload
- three-taper bore, 50 percent preload, loose clearances
- three-taper bore, 50 percent preload, tight clearances
- three-axial groove, 0 percent preload, normal clearances
- three-axial groove, optimum preload (0 percent), clearance, θ_p (angular orientation), and θ_c (angular extent of axial oil feed grooves)

The key to optimizing mechanical performance for the compressor rotor is to reduce the average bearing stiffness as much as possible in order to reduce the high amplification through the critical as well as improve running speed damping characteristics. This is accomplished by removing the node points in the dynamic mode shapes as far as possible from the rotor's radial bearing locations.

This is necessary since the controlling factor in the dynamics of the subject rotor is the very high ratio of bearing stiffness to shaft stiffness. The ratio of bearing span to midspan diameter = 10.4 while the journal bearings are heavily loaded, rendering them very stiff in the load direction for all bearing designs.

It thus becomes necessary to design for minimal stiffness in the no-load direction in order to optimize shaft dynamics, response and stability.

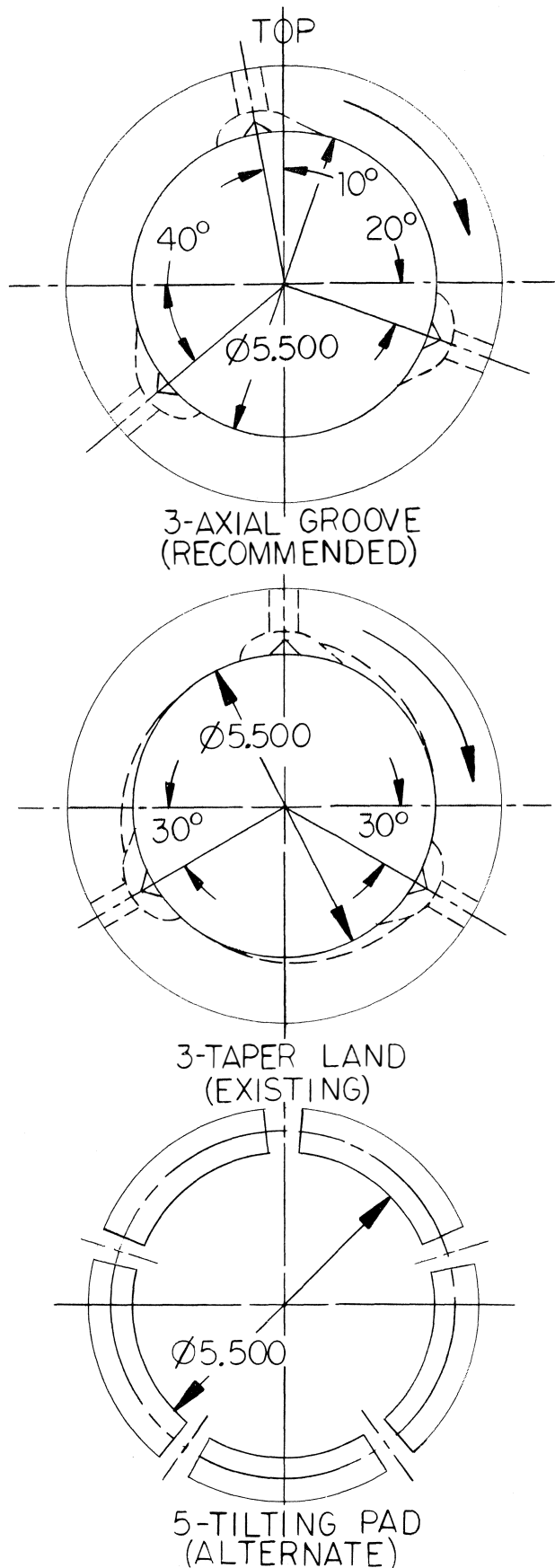
Detailed results are presented for (Figure 37):

- existing three-lobe bearing insert design
- alternate five-tilting pad bearing design (optimized)
- recommended three-axial groove plain bearing design (optimized) of which the 3-AG design is superior for this application. Other design alternatives offered no significant improvement over these basic configurations.

A comparison of X-direction bearing stiffness yields the following summary:

Design	K_x
3-Axial groove	410,000 lb/in—most desirable
Existing 3-Lobe	830,000 lb/in
5-Tilting shoe	1,600,000 lb/in—least desirable

It should be noted that the bearings analyzed were individually optimized for this compressor application. For the case of the 5-tilting shoe design, for example, a maximum length bear-



ing was fit to the rotor with a minimum advisable preload, $\delta = 30$ percent, for best performance and minimum stiffness.

Dynamic Response to Rotor Unbalance

Results of the rotordynamic response and stability analysis demonstrate that, as compared with the existing bearing design, tilting-pad bearings greatly degrade dynamic performance, while the proposed new plain insert design significantly enhances its dynamic characteristics.

The vertical component of the rotor's first critical is at 2200 cpm with $AF = 22$ for all bearing designs. This is due to high bearing stiffness in the load direction, which is not sensitive to bearing design alone.

The horizontal component(s) of the rotor's first critical or first peak response frequency, $1PRF(1)$, along with its attendant amplification factor for the given bearing designs are:

Design	$1PRF(1)$	AF
3-Axial groove	1500 cpm	8
Existing 3-Lobe	1700 cpm	13
5-Tilting shoe	2100 cpm	21

Reduction in frequency and amplification factor for this modal component is significant relative to greatly improved stability for the forward whirl mode which is sensitive to aerodynamic excitation. (The 2200 cpm component is an instability mode for a backward whirl excitation mechanism, such as a self-sustaining rotor rub).

The rotor's split components of the second critical, $2PRF(1)$ and $2PRF(2)$, give further evidence of improvement via support stiffness reduction for both X, and Y, direction controlled modes:

Design	$2PRF(1)$	$2PRF(2)$
3-Axial groove	3800 cpm	6150 cpm
Existing 3-Lobe	5000 cpm	6250 cpm
5-Tilting shoe	5700 cpm	6650 cpm

The second critical amplifies above 6000 rpm for all cases (Y-component) while the X-component is critically damped, but is of significance in demonstrating improved damping capacity of the lower frequency modes, i. e., the bearing designs that generate those particular modes.

It is significant to note that while the insert bearing designs, both existing and proposed, generate less horizontal damping than does the optimized five-tilting shoe design, when coupled with the reduction in horizontal stiffness, yield a net significant increase in the effective or usable damping provided to the rotating system.

\bar{K}_x and \bar{K}_y , ratios of bearing stiffness to shaft stiffness in the X and Y directions, respectively, have been calculated for the optimization study:

Design	\bar{K}_x	\bar{K}_y
3-Axial groove	1.83	11.19
Existing 3-Lobe	3.70	8.84
5-Tilting shoe	7.16	12.53

The improvement achieved in this design parameter by the plain insert bearings is clear. A good design minimizes \bar{K} , where any value of \bar{K} above five or six indicates a detrimental rigid bearing flexible shaft condition. Thus, it is in the X-direction that a real improvement is had with an optimized three-axial groove insert bearing. Conversely, it can be seen that a tilting-pad bearing is highly undesirable.

Vibration amplitudes at the rotor midspan (in the critical, distributed unbalance) and normalized sensitivities are as follows:

Figure 37. Bearing Design Alternatives—Optimization Study.

Design	Vibration Amplitude, A	Normalized Sensitivity, S
3-Axial groove	3.16 mils	80%
Existing 3-Lobe	4.5 mils	100%
5-Tilting shoe	4.25 mils	95%

Thus, the expected improvement in vibration response for the rotor's first bending mode at the point of maximum amplitude.

Representing perhaps the most significant aspect of this bearing design optimization study is the comparison of running speed rotor displacements at the bearings, $U = 56,347 \text{ W/N}^{0.2}$ oz-in (distributed unbalance), and normalized sensitivities:

Design		Vibration Amplitude, A	Normalized Sensitivity, S
3-Axial groove	Brg. #1	.36 mils	120%
	Brg. #2	.30 mils	100%
Existing 3-Lobe	Brg. #1	.30 mils	100%
	Brg. #2	.30 mils	100%
5-Tilting shoe	Brg. #1	.05 mils	16%
	Brg. #2	.02 mils	6%

These analytical results clearly demonstrate the unacceptable dynamic characteristics of the tilting-shoe (optimized) journal bearing design for this application, as this design results in node points at the bearings at normal operating speed. Alternatively, the optimized insert bearing design offers a significant improvement over the existing design.

Severe nodal points at a machine's radial bearings at running speed results in poorly damped vibration response and the resulting undesirable mechanical performance.

In addition to the foregoing, dynamic analysis is due consideration of past experience with machines which are mechanically similar to the subject propylene compressor and which exhibit identical rotordynamic characteristics. Operational experience with these machines has demonstrated:

- undesirable machine vibration using tilting-shoe bearings.
- favorable operation with optimized three-axial groove insert bearing designs.

The inclusion of "differential fits" for the new impeller designs in the first four stages of the rerated machine will certainly also aid in avoiding vibration problems due to the very long bearing span and the resultant rotor flexibility.

It is significant to note that the existing bearing inserts, being of taper bore design, can perform significantly worse than the present analysis indicates, as this design is especially sensitive to manufacturing tolerances and errors as reported by Kirk [5].

Rotor Bearing System Stability

The principal results of the rotor stability analysis for the bearing optimization study are as follows (rotor speed = 4700 rpm):

Design	Log Dec, δ_0	Damped Frequency, f_n	Nonsynchronous Amplification Factor, AF
3-Axial groove	+ .361	1550 cpm	8.74
Existing 3-Lobe	+ .235	1710 cpm	13.40
5-Tilting shoe	+ .146	2130 cpm	21.50

These parameters define the forward whirl instability. While the existing three-lobe design has a finite stability threshold (Figure 38), the optimized insert design and tilting-pad designs have infinite threshold speeds.

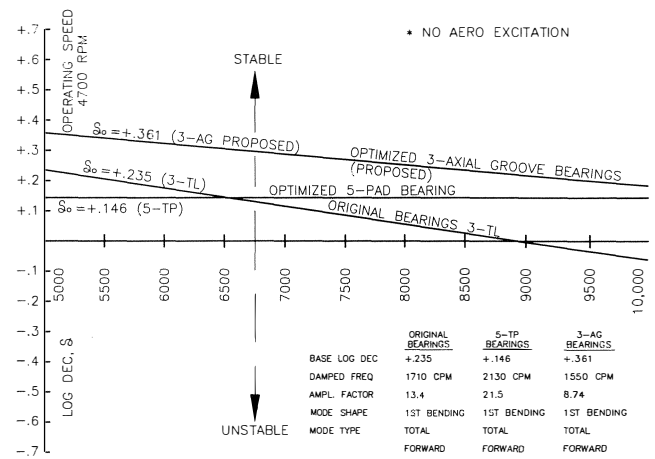


Figure 38. Compressor Rotor Stability—Optimization Study.

While the proposed three-groove insert design has an infinite stability threshold, i. e., it is not subject to fractional frequency oil whirl, the machine log decrement, δ , then becomes a measure of the rotor's resistance to shaft whip at the fundamental resonance due to undesirable levels of shaft flexibility. In this regard, the proposed insert bearings optimize not only rotor response, but stability as well.

Contributing to overall improvement in system stability is the asymmetry of the stiffness characteristic generated in the X and Y directions by the optimized insert bearings.

As the propylene compressor is not a high energy density machine, it is not expected to experience high levels of aerodynamic excitation. Also, since suction pressure is not high, cone oil seal contributions to rotor instability are negligible.

The 2200 cpm frequency common to all bearing design applications for this rotor becomes the reverse precession instability mechanism which could be excited subsynchronously, for example, by a severe rotor rub condition. This condition would be common to all bearing designs, as it is a characteristic of the Y-direction dynamics.

Conclusions

- The propylene compressor rotor's critical speeds occur at $Nc1 = 2200 \text{ rpm}$ and $Nc2 = 6200 \text{ cpm}$.
- The most significant aspect of the unit's rotordynamics characteristics is the high amplification factor (AF) of the first critical, $AF = 22$, indicative of a highly amplified pure rotor first bending mode (with rigid bearings), which is conducive to undesirable dynamics and stability characteristics.
- Bearing design optimization studies, summarized in Table 5, confirm that five-tilting pad type bearings for this application are extremely undesirable, optimized tilt-pad bearings generat

Table 5. Summary of the Bearing Design Optimization Study for a Propylene Refrigeration Compressor.

Bearing Type	Hydrodynamic Bearing Coefficients @ Design Speed Existing Pressure Dam vs. Retrofit 5-Tilting Pad			
	Kxx (Lb/In)	Kyy (Lb/In)	Cxx (Lb-Sec/In)	Cyy (Lb-Sec/In)
Existing P-Dam	400,000	2,000,000	580	3,300
Retrofit 5-Pad	1,000,000	1,100,000	2,800	6,600

ing too much stiffness for the compressor rotor, resulting in unacceptable mechanical performance both at normal operating speed and in the critical.

- An optimized three-axial groove insert bearing design is shown to demonstrate superior dynamics and stability characteristics over a wide range of manufacturing tolerances. The proposed insert bearing design is considered the bearing of choice for this particular application, not only by analysis, but from experience.

- Startup and operation on the redesigned bearings has been highly successful, the rotor operating with very low vibration levels, and running smoother than it ever ran before the rework.

SUMMARY AND CONCLUSIONS

The machinery case histories detailed herein illustrate some of the variety and subtlety of design problems encountered in existing rotating machinery and their engineering resolutions, including upgrade and redesign. A significant purpose of the technical information presented here is to help in avoiding improper diagnosis and treatment of machinery design problems by treating them as recurring maintenance problems. This common misdiagnosis continues to result in unnecessary maintenance expense and very costly downtime.

Examples of the common requirement for proper redesign are demonstrated in the areas of:

- machinery built before the development of today's powerful design tools in the areas of rotordynamics and bearing design.
- marginal machines that operate satisfactorily until they are rerated, their greater output resulting in the need for mechanical upgrade.
- poorly designed or improperly designed aftermarket or OEM parts that have been retrofitted to existing machines.
- units that can be improved via design optimization in order to enhance future operational reliability.
- analytical design studies that uncover potential future operational machine problems.

The documented case histories deal with a variety of machinery design problems including gear design, gearbox bearing design, gas compressor bearing redesign as part of a performance upgrade, steam turbine bearing redesign to obtain unit reliability, an operations approach to rotordynamics optimization of a high pressure barrel compressor, rotor assembly redesign to stabilize the rotor build of a high temperature NO_x module, nitric acid expander bearing redesign for system stability and reliability, large induction motor starting circuitry transients and problem resolution, and refrigeration compressor bearing design optimization study demonstrates the significant disadvantages of five tilting pad bearings for that application.

REFERENCES

1. Lifson, A., Simmons, H. R., and Smalley, A. J., "Vibration Limits for Rotating Machinery," *Mechanical Engineering*, pp. 60-63 (June 1987).
2. Nicholas, J. C., "Pressure Dam Bearing Design for Optimum Turbomachinery Stability," *Hydrocarbon Processing*, pp. 91-97 (April 1983).
3. Mondy, R. E., and Mirro, J., "The Calculation and Verification of Torsional Natural Frequencies for Turbomachinery Equipment Strings," *Proceedings of the Eleventh Turbomachinery Symposium*, Turbomachinery Laboratory, Department of Mechanical Engineering, Texas A&M University, College Station, Texas, pp. 151-156 (1982).
4. American Petroleum Institute, "Centrifugal Compressors for General Refinery Services," API Standard 617, 5th Edition, (1988).
5. Kirk, R. G., "The Influence of Manufacturing Tolerances on Multi-Lobe Bearing Performance in Turbomachinery," *Topics in Fluid Film Bearing and Rotor Bearing System Design and Optimization*, an ASME publication, pp. 108-129 (April 1978).

